

國立臺灣大學理學院地理環境資源學系



學士論文

Department of Geography

College of Science

National Taiwan University

Bachelor's Thesis

臺灣高山河川無機氮輸出控制因子之交互作用：

獨特的氣候系統與不可忽視的人類－地景系統

Interactive Control of Climatic System and  
Human-Landscape System on Riverine DIN Export in  
Small Mountainous Rivers of Taiwan

李玟璇

Wen-Shiuan Lee

指導教授：黃誌川 博士

Advisor: Jr-Chuan Huang, Ph.D.

中華民國 110 年 4 月

April 2021

國立臺灣大學學士班學生論文  
口試委員會審定書

臺灣高山河川無機氮輸出控制因子之交互作用：  
獨特的氣候系統與不可忽視的人類-地景系統  
Interactive Control of Climatic System and  
Human-Landscape System on Riverine DIN Export in  
Small Mountainous Rivers of Taiwan

本論文係李玟璇君(B06208033)在國立臺灣大學地理環境資源學系完成之學士班學生論文，於民國110年04月23日承下列考試委員審查通過及口試及格，特此證明

口試委員：

黃誌川

(簽名)

(指導教授)

李厚福


張仲德

系主任：

(簽名)

(是否須簽章依各院系規定)

## 謝 誌



這份論文的能夠完成，要感謝許多人一路上對於我實質或是精神上的協助。首先，特別感謝我的指導教授黃誌川老師，從我大二進入研究室至今，在學術、課業與以及其他許多方面的指導，鼓勵我參與許多課外活動，從科技部大專生計畫、交換生計畫到學士論文競賽都給我許多珍貴的建議與協助，帶著我突破重重難關。謝謝張仲德老師，總是不辭辛勞地給予我最及時的建議並不厭其煩地協助我修改文章，讓我的研究成果在兩位老師的協助下得以被刊登在期刊中。謝謝口試委員李宗祐老師給予我的建議與肯定。

謝謝研究室的大家，很开心在大學的生活中有超過一半的時間都是與你們一起度過，一起出野外、聚餐、去東澳划獨木舟看日出都是我大學中很美好的回憶。謝謝何爸，總是加班協助、教導我們，答應我們無理的要求，幫助我完成許多不可能的任務。謝謝很單的孟璋學長在我整個研究中從分析到繪圖給予了莫大的協助，謝謝庭彰學長在我進入研究室初期給予的指導。謝謝偉倫能者多勞地扛起許多責任並在第一時間協助我解決所有儀器的疑難雜症，謝謝郁昕、芳慈，在大二還懵懵懂懂之時拉著我一起進入研究室，三個小蘿蔔頭就這樣一起走過了三年，成為我最重要的精神資助。謝謝賈伯總是帶給研究室許多歡笑還教了我們無數次的水文模式，謝謝俐瑾、啟見、恩如、菲菲、老大、沛壕、易哲還有所有曾經待過研究室的大家，不厭其煩地陪我進行一次次的報告預演，並給我最真摯的建議，即使是當我在德國交換，兩地有著時差的情況下也毫不例外，讓我有信心完成一次次的挑戰。在進入研究室前，我從未想過我的大學生活可以如此精彩充實，並有機會獲得我如此隆重的肯定，雖然中間過程很辛苦，但一切依然值得。

謝謝地理系 B06 的同學們，縱使我並沒有經常參與系上活動，但每次相遇總能感受到溫暖地問候與寒暄。謝謝僑生團，為我在系上的生活添加了許多樂趣。謝謝我的室友怡玆陪伴我度過無數個寫論文崩潰的夜晚，能夠成為你的室友是我大學中最幸運的事情，謝謝子芸、以瑄還有多位多年老友一路的陪伴。

感謝我的家人，謝謝我的爸媽、姊姊、哥哥總是無條件地相信我、包容我、支持我的決定，給予我最自由的發展空間，在我低潮時成為最溫暖的避風港。

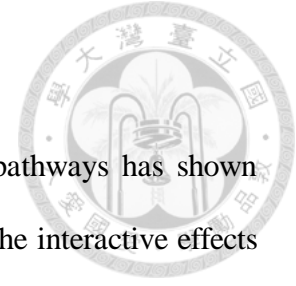
最後，我期許自己能夠繼續保持熱情，持續精進各項能力，不辜負自己以及他人對於我的肯定與期待，並且永遠記得當個溫暖並懂得感恩的人。

## 摘要

幾十年來，陸域水體的氮循環在不同途徑的人為添加的干擾下已經產生顯著地變化，但是河川中溶解性無機氮(DIN)輸出的重要控制因子(如：氣候、地貌、人為活動等)彼此之間的交互作用至今仍不清楚。本研究針對全台灣四十三個集水區，流域面積涵蓋全島 71%，進行兩年的月採樣(2015-2016)分析 DIN 物種濃度( $\text{NO}_2^-$ ,  $\text{NO}_3^-$ , and  $\text{NH}_4^+$ )。其後，以偏冗餘分析法(partial redundancy analysis)探討這些環境因子彼此之間的交互作用對於河川中溶解性無機氮輸出的影響。結果顯示，臺灣每年河川中溶解性無機氮輸出量約為  $3100 \text{ kg-N km}^{-2} \text{ yr}^{-1}$ ，變化幅度從人為干擾較少的台灣東部( $\sim 230 \text{ kg-N km}^{-2} \text{ yr}^{-1}$ )至台灣西南部與北部等人為干擾程度較高的流域( $\sim 10000 \text{ kg-N km}^{-2} \text{ yr}^{-1}$ )。硝酸鹽( $\text{NO}_3^-$ )通常為河川中溶解性無機氮的主導成分，然而銨( $\text{NH}_4^+$ )在受人為干擾的流域中也具有重要的貢獻。除了地貌因子(如坡度、面積、河道長度)與河川中溶解性無機氮輸出呈現負相關外，其餘環境變數皆與河川中溶解性無機氮輸出呈現為正相關。季節方面，濕季時，氣候與人為活動-地景(LH)因子間的相互關係不明顯，各自對於硝酸鹽輸出產生影響，但在乾季時，氣候-人為活動(CH)因子則共同控制硝酸鹽輸出。無論乾濕季，銨主要受人為活動-地景(LH)因子所控制。但乾季時，人為活動因子對於銨輸出的的影響力較低。整體而言，控制因子對於河川中溶解性無機氮輸出會因種類和季節而異，因此針對水質相關管理措施，未來在設計時也應該將這些因素納入考量。

**關鍵字：**溶解性無機氮、冗餘分析、偏冗餘分析、山地小河流、臺灣

## Abstract



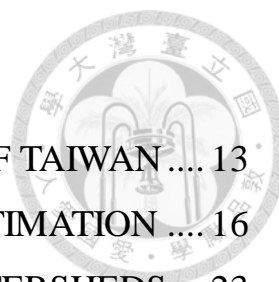
Increasing anthropogenic nitrogen (N) emission via different pathways has shown prominent impact terrestrial and aquatic ecosystems for decades, but the interactive effects among climate-, landscape- and human-associated variables on riverine DIN (dissolved inorganic nitrogen, mainly  $\text{NO}_2^-$ ,  $\text{NO}_3^-$  and  $\text{NH}_4^+$ ) export are unclear. In this study, the samples from 43 watersheds with a wide range of climate-, landscape- and human-associated gradients across Taiwan were collected and analyzed. Further, the partial redundancy analysis (pRDA) was applied to examine their interactive controls on riverine DIN export. Results show that the annual riverine DIN export in Taiwan is approximately  $3100 \text{ kg-N km}^{-2} \text{ yr}^{-1}$ , spanning from  $230 \text{ kg-N km}^{-2} \text{ yr}^{-1}$  in less disturbed watersheds (eastern and central Taiwan) to  $10,000 \text{ kg-N km}^{-2} \text{ yr}^{-1}$  in watersheds with intensive human intervention (southwestern and northern Taiwan).  $\text{NO}_3^-$  is generally the single dominant form of DIN, while  $\text{NH}_4^+$  renders significance in disturbed watersheds.  $\text{NO}_3^-$  exports in the wet season were controlled by climate and human-landscape variables independently, yet in the dry season climate-human variables jointly dominate  $\text{NO}_3^-$  export. Meanwhile, human-landscape (LH) variables control  $\text{NH}_4^+$  exports in both seasons. Precisely, the contributions of controlling variables on DIN export vary with species and seasons, indicating water quality management could be time-dependent, which should be taken into consideration for designing mitigation strategies.

**Keywords:** dissolved inorganic nitrogen (DIN); redundancy analysis (RDA); partial redundancy analysis (pRDA); small mountainous rivers (SMRs); Taiwan

## CONTENTS

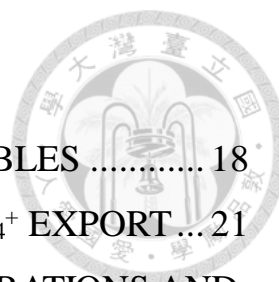
謝 誌 .....	2
摘 要 .....	3
ABSTRACT.....	4
1. INTRODUCTION .....	8
2. MATERIALS AND METHODS .....	10
2.1. N CYCLE.....	10
2.2. DIN IN TAIWAN .....	11
2.3. STUDY SITE .....	11
2.4. DIN SAMPLING AND STREAMFLOW SIMULATION .....	13
2.5. EXPORT ESTIMATION.....	14
2.6. VARIATION PARTITIONING: PCA, RDA AND PRDA.....	17
3. RESULTS .....	22
3.1. RIVERINE DIN CONCENTRATION AND EXPORT .....	22
3.2. SCATTERPLOT MATRIX .....	25
3.3. PCA OF ENVIRONMENTAL VARIABLES.....	27
3.4. VARIANCE PARTITIONING—RDA AND PRDA.....	29
4. DISCUSSION .....	33
4.1. CHARACTERISTICS OF DIN CONCENTRATIONS AND EXPORTS IN TAIWAN .....	33
4.2. INFLUENCES OF MAIN VARIABLES AND THEIR INTERACTIVE EFFECTS ON DIN EXPORT .....	34
4.2.1. CLIMATIC CONTROL.....	34
4.2.2. THE CONSIDERATION OF LANDSCAPE AND BUFFER ZONE .....	35
4.2.3. HUMAN DISTURBANCE.....	37
4.2.4. INTERACTIVE EFFECTS AMONG VARIABLES.....	38
5. CONCLUSIONS .....	40
REFERENCES .....	42
SUPPLEMENTARY MATERIALS.....	48





## LIST OF FIGURES

FIGURE 1. STUDY SITES AND LAND COVER MAP OF TAIWAN ....	13
FIGURE 2. THE MODELS USING IN THE EXPORT ESTIMATION ....	16
FIGURE 3. DIN, NO <sub>3</sub> <sup>-</sup> AND NH <sub>4</sub> <sup>+</sup> EXPORTS OF 43 WATERSHEDS ...	23
FIGURE 4. MONTHLY NO <sub>3</sub> <sup>-</sup> AND NH <sub>4</sub> <sup>+</sup> EXPORTS IN TWO SITES ....	24
FIGURE 5. SCATTERPLOT MATRIX AMONG ENVIRONMENTAL FACTORS, NO <sub>3</sub> <sup>-</sup> , NH <sub>4</sub> <sup>+</sup> AND DIN EXPORTS.....	26
FIGURE 6. PCA OF ENVIRONMENTAL VARIABLES FOR STUDY SITES FOR NO <sub>3</sub> <sup>-</sup> AND NH <sub>4</sub> <sup>+</sup> EXPORT.....	28
FIGURE 7. SEASONAL VARIANCE DECOMPOSITION OF NO <sub>3</sub> <sup>-</sup> EXPORTS IN 43 WATERSHEDS.....	31
FIGURE 8. SEASONAL VARIANCE DECOMPOSITION OF NH <sub>4</sub> <sup>+</sup> EXPORTS IN 43 WATERSHEDS.....	32



## LIST OF TABLES

TABLE 1. DEFINITION OF ENVIRONMENTAL VARIABLES .....	18
TABLE 2. EIGENVALUES OF PRDA OF $\text{NO}_3^-$ AND $\text{NH}_4^+$ EXPORT ...	21
TABLE 3. MEAN ESTIMATED SEASONAL CONCENTRATIONS AND EXPORTS.....	23
TABLE 4. THE MARGIANL EFFECTS AND TOTAL INERTIA OF ENVIRONMENTAL VARIABLES ON $\text{NO}_3^-$ AND $\text{NH}_4^+$ EXPORTS.....	29

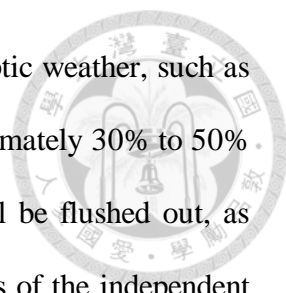




## 1. Introduction

Reactive nitrogen, a vital and essential nutrient for organisms and ecosystems, plays a key role in maintaining biodiversity and functions of ecosystems (e.g. Aber et al., 1998; Galloway et al., 2004). Over the past half century, the rapid increasing anthropogenic N emissions inevitably accelerated N deposition into the biosphere (Seitzinger et al., 2010), and consequently exceeded the N-requirement for terrestrial ecosystems (Rockström et al., 2009). Studies show that N emissions and depositions have been declining in Europe and the U.S. since 2000. East and South Asia, in contrast, have become the hot spots of pollutant emissions due to population growth and intense agricultural activities (Tørseth et al., 2012; Vet et al., 2014). Regions located near the emission source of East Asia receive excessive N deposition under favorable climatic conditions, such as the East Asian monsoon that blows directly to Taiwan with abundant rainfall (Chang et al., 2000). The overloaded dissolved inorganic nitrogen (DIN) (majorly  $\text{NO}_3^-$ , and  $\text{NH}_4^+$ ) potentially led to eutrophication and harmful algal blooms which deteriorated water quality and caused damages in aquatic communities (Conley et al., 2009). However, the DIN exports, particularly for seasonal changes, in subtropical mountainous watersheds are still unclear.

Many studies have demonstrated that even a mild replacement of natural vegetation with agricultural land use within watersheds would have significant impacts on hydro-chemical processes (Howarth et al., 2012; Chang et al., 2018), especially for DIN export from non-point pollution sources (Huang et al., 2012, 2016; Lee et al., 2013). Landscape features such as slope, soil type/moisture, channel length, watershed area and relief also regulate water quality (Sliva and Williams, 2001). In addition, climatic factors play a principal role in nutrient cycling in the era of warming climate and increasing extreme events. A warmer temperature will accelerate biogeochemical processes that would alter enzyme reactions, e.g., nitrification and denitrification, via microbial activities



(Pajares and Bohannan, 2016). The torrential rainfall caused by synoptic weather, such as thunderstorms and tropical cyclones during summer, can bring approximately 30% to 50% of annual precipitation, such that a considerable amount of DIN will be flushed out, as evidenced in Taiwan (Huang et al., 2012, 2016). However, the effects of the independent and interactive relationship among landscape patterns, climatic factors and anthropogenic disturbance are still not clear on riverine DIN export (Howarth, 1998).

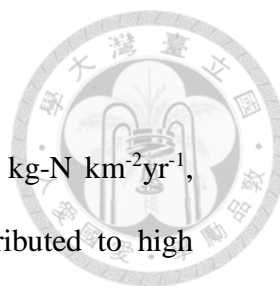
Previous analyses widely used linear or non-linear regression models to estimate the DIN export, but failed to separate the collinearity among variables, which might violate the statistical independent assumption (Graham 2003). To tackle the issues of collinearity, a series of well-developed methods, namely, principal components analysis (PCA), redundancy analysis (RDA) and partial RDA (pRDA), have been utilized to clarify the relative importance of independent variables and their interactive effects on dependent variables (ter Braak, 1988; Borcard et al., 1992). In this study, we apply PCA and pRDA to evaluate the contribution of climatic-, landscape- and human-associated variables and their interactions on DIN export based on 43 island-wide watersheds in Taiwan. This synthesis can help to disentangle the intertwined effects of these fundamental environmental factors on the behaviors of nutrient fluxes. Specifically, the objectives of this study are to (1) quantify riverine DIN export in subtropical watersheds in Taiwan, (2) explore the interplay of human disturbance, climatic factors and landscape characteristics on riverine  $\text{NO}_3^-$  and  $\text{NH}_4^+$  exports, respectively, and (3) figure out the spatial and seasonal variation of the controlling factors' influences on DIN exports.



## 2. Materials and Methods

### 2.1. N Cycle

Nitrogen (N) is a common limiting nutrient element in many ecosystems, availability of N plays a key role in characterizing biodiversity and ecosystem function (Aber, 1989; Aber et al., 1998). More than 99% of the N cannot be directly used by more than 99% of living organism (Galloway et al., 2003). Most of N in the atmosphere exists in the form of  $N_2$ , which cannot be used for most organisms. As result, in the process of nitrogen fixation provide a path for converting  $N_2$  into reactive nitrogen, which is available to most living organisms. Although most nitrogen fixation is carried out by some microbes, some nitrogen can be fixed by lightning or certain industrial processes, including the combustion of fossil fuels and the Haber-Bosch process since the early 20<sup>th</sup> century. In riverine systems, N species can be classified into PN (particulate nitrogen), DON (dissolved organic nitrogen), and DIN (dissolved inorganic nitrogen, including  $NO_2^-$ ,  $NO_3^-$ , and  $NH_4^+$ ), among which DIN comprises the majority of total riverine N in most rivers (Galloway et al., 2004; McCrackin et al., 2014). The process that converts organic N to ammonium ( $NH_4^+$ ) is known as mineralization. Ammonium ( $NH_4^+$ ) would be oxidized to nitrite ( $NO_2^-$ ) and nitrate ( $NO_3^-$ ) by certain bacteria and archaea in the process called nitrification. The pathways that N leaves the soils are complicated and related to microbial biochemical process, including plant uptake or leaching into streams or deeper zone. Besides, denitrification is also a pathway of N removal, which microbes reduce  $NO_3^-$  to  $NO$ ,  $N_2O$  and then  $N_2$ .



## 2.2. *DIN in Taiwan*

In previous study, Taiwan has high riverine DIN export  $\sim 3800 \text{ kg-N km}^{-2}\text{yr}^{-1}$ , which is  $\sim 18$  times higher than the global average, and it is attributed to high atmospheric N deposition ( $\sim 2000 \text{ kg-N km}^{-2}\text{yr}^{-1}$ ), heavy fertilizer applications, and large human waste emissions (Huang et al., 2016). This pattern and levels of DIN exports consist of results reported for over 20 sub-catchments within two river networks in northern and central Taiwan (Huang et al., 2012, Lee et al., 2014). However, the DIN export varies considerably due to the extent of disturbance on watersheds (Huang et al., 2016). Annually, 3-5 typhoons invade Taiwan during June to October and can contribute 20–70% of the annual DIN export of river in Taiwan (Huang et al., 2012). Notably,  $\text{NO}_3^-$  is the dominant species for low and moderately disturbed watersheds but  $\text{NH}_4^+$  is the dominant species, accounting for more than 50% of annual DIN export for highly disturbed watersheds (Huang et al., 2016).

## 2.3. *Study Site*

Taiwan, located in the northwest Pacific Ocean, is a tropical/subtropical mountainous island in the East Asian monsoon climate zone. Elevation ranges from sea level to approximately 4000 m in a short horizontal distance ( $< 75 \text{ km}$ ). The Tropic of Cancer crosses the central part of Taiwan, which divides the island into tropical monsoon climate in the south and subtropical monsoon climate in the north. The mean annual temperature (MAT) is  $22 \text{ }^\circ\text{C}$  across the island, ranging from  $15.0 \text{ }^\circ\text{C}/18.2 \text{ }^\circ\text{C}$  in the north/south in January to  $28.7 \text{ }^\circ\text{C}/28.4 \text{ }^\circ\text{C}$  in July, and the MAT decreases with increasing altitude (Chang et al., 2014). The mean annual precipitation (MAP) is 2500 mm for the entire island but shows high spatial variability ranging from less than 1500 mm in southwest Taiwan to over 4000 mm in the mountains of northeastern Taiwan (Chang et al., 2014).

There are more than 75% of MAP falls in the humid summer (May to October), while winter–spring (November to April) is a relatively dry period.

Natural forests, plantation and bamboo forests cover 60% of the land, while farmlands and urbanized areas occupy 29% and 11%, respectively (Figure 1). The dominant vegetation types and land cover of Taiwan change from mixed and conifer forests at the mid and high elevation (>2000 m a.s.l.), evergreen broadleaf forests at the low and mid elevation (200–2000 m a.s.l.) to urban, buildup area and farmland on coastal plains (<800 m a.s.l.) (Figure 1). In this study, in order to estimate island-wide watershed DIN export, our sampling scheme covers a total of 43 sites. Individual watershed represented by each site can be as small as 82 km<sup>2</sup> and as large as 2969 km<sup>2</sup>, and as a whole, they occupy more than 70% of the island and distribute evenly across Taiwan (Figure 1). Twenty-nine of the 43 watersheds are majorly covered by natural forest (>70% of forest cover), while 14 of the 43 are situated in the transition between mountain and plain regions where agricultural land cover and buildup area account for 10–65% and 0–18%, respectively (Figure 1 and Table S1). The average slope of the watersheds varies from 8% to 76%.

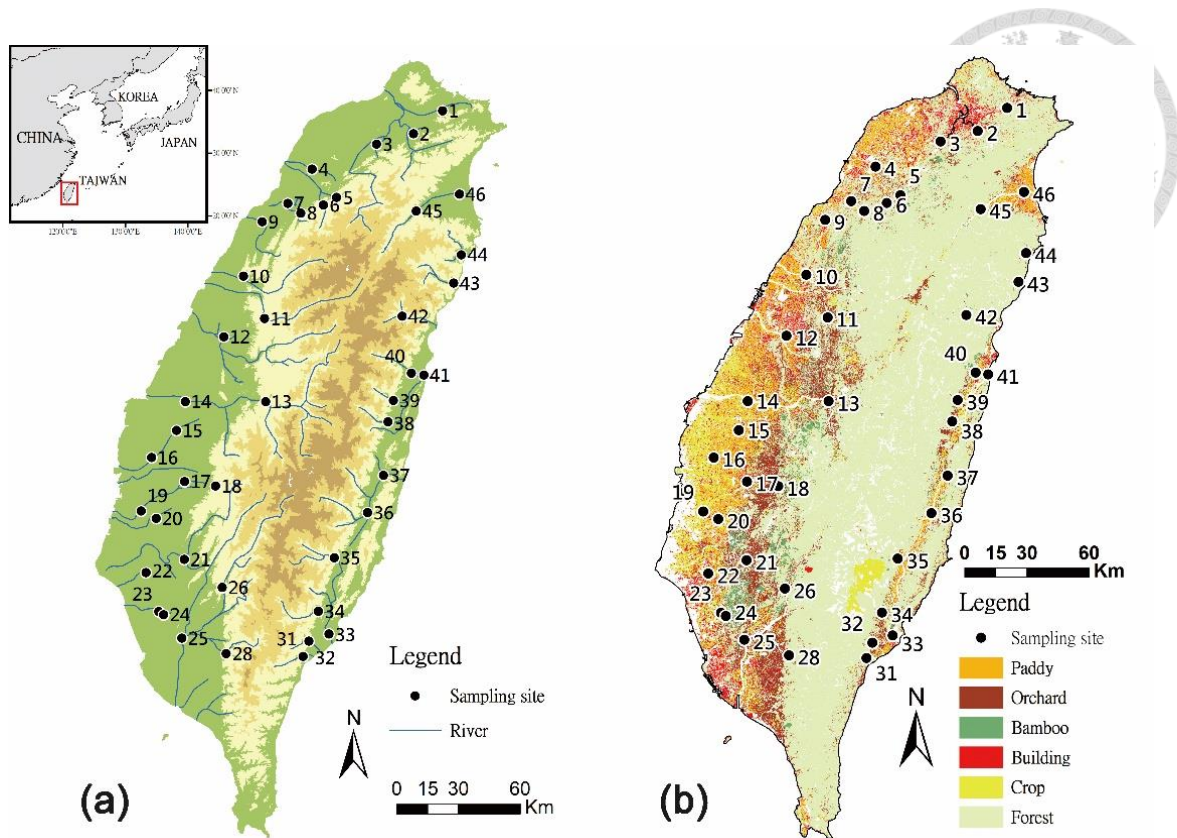
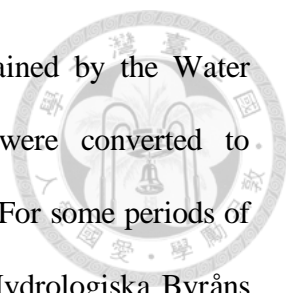


**Figure 1.** The geographical location of 43 sampling sites (a) and land cover map of Taiwan (b).

#### 2.4. DIN Sampling and Streamflow Simulation

A monthly sampling scheme was conducted at all sampling sites (watersheds) during 2015–2016. Each route would be finished within 2 days. Stream water samples were collected by plunging a 1-L PE (polyethylene) bucket into stream, and the water was immediately filtered through 0.7  $\mu\text{m}$  filters. A 15 ml subsample of filtrate was frozen on-site in liquid nitrogen and kept frozen until laboratory analysis at National Taiwan University. Nitrate, nitrite and ammonium content were analyzed using ion chromatography (IC) using a Dionex ICS–1500 (Thermo Fisher Scientific Inc.® Sunnyvale, CA, USA) with a detection limit of 0.2, 0.2, and 0.4  $\mu\text{M}$ , respectively. Our DIN calculation includes  $\text{NO}_2^-$ ,  $\text{NO}_3^-$  and  $\text{NH}_4^+$ . Among them, nitrite is easily oxidized to nitrate and accounts for a small fraction (<5.0%). Therefore, we mainly analyzed and discussed  $\text{NO}_3^-$  and  $\text{NH}_4^+$ .



Streamflow was acquired from the water level stations maintained by the Water Resource Agency ([www.wra.gov.tw](http://www.wra.gov.tw)). The water level records were converted to streamflow via an individual rating curve and cross section approach. For some periods of missing records and ungauged sites, a hydrologic model (HBV, the Hydrologiska Byråns Vattenbalansavdelning model) (Parajka et al., 2013) was used to fill the data gaps (Huang et al., 2011). The historical observed daily streamflow was utilized to train the parameter set to fit low, normal, and extreme values of simulated streamflow using the performance measure of NSE (Nash-Sutcliffe efficiency coefficient) (Nash and Sutcliffe, 1970). The calibrated parameter set was then applied to the watersheds using their own climatic inputs and terrain information to simulate their daily streamflow during 2015–2016.

### *2.5. Export Estimation*

Based on the discrete  $\text{NO}_3^-$  and  $\text{NH}_4^+$  concentration and continuous streamflow rates, individual  $\text{NO}_3^-$  and  $\text{NH}_4^+$  export of the 43 sites were then estimated using an R software package, *loadflex*, which provides several common methods (e.g., interpolations, regressions and composite method) for export estimation (Appling et al., 2015). The composite method synthesizing rectangular interpolation and regression models is applied for export estimation. The mean values of two export methods in 2015 and 2016 were used as export results for further analysis. The rectangular interpolation has usually been used for studies on solute and sediment exports, where horizontal lines are drawn through observations in a plot of concentrations against time, and each horizontal line is connected to the next by a vertical line midway between successive observations (Porterfield, 1972). The regression approach is a longstanding interpolation in estimating watershed solute exports (Figure 2). It often requires less data than other models if the data can span over the range of predictors instead of the full time period of interest (Robertson and Roerish, 1999). A simple regression equation based on observed nutrient concentrations and concurrent

streamflow (Q) with an exponent function is used to represent the hydrological influence on transport as Equation (1) below:

$$EXPORT = m \sum_{j=1}^T Q_j C_j = m \sum_{j=1}^T Q_j e^{a_0 + a_1 \ln Q_j}, \quad (1)$$

where  $Q_j$  [ $\text{mm d}^{-1}$ ] is the daily streamflow rate on j-th day;  $C_j$  [ $\text{mg-N L}^{-1}$ ] is an estimated concentration of  $\text{NO}_3^-$  and  $\text{NH}_4^+$  on the j-th day, m is the conversion factor to convert the calculated values into a specific unit [ $\text{kg-N km}^{-2} \text{yr}^{-1}$ ], and  $a_0$  and  $a_1$  are regressive coefficients. Coefficient  $a_0$  is generally highly associated with the mean of observed nutrient concentration, and  $a_1$  indicates the hydrological influence. A larger coefficient,  $a_1$  ( $>0$ ), indicates enhanced concentration with increasing streamflow, whereas a smaller value reflects the dilution effect because concentration decreases with the increase of discharge percentage. From Equation (1), we can estimate the concentration and export for non-measured days by introducing continuous daily streamflow (Ferguson, 1986). According to the hydrologic seasonality, we summarized the daily export from May to October as wet season export and the summation of other daily exports as dry season export.



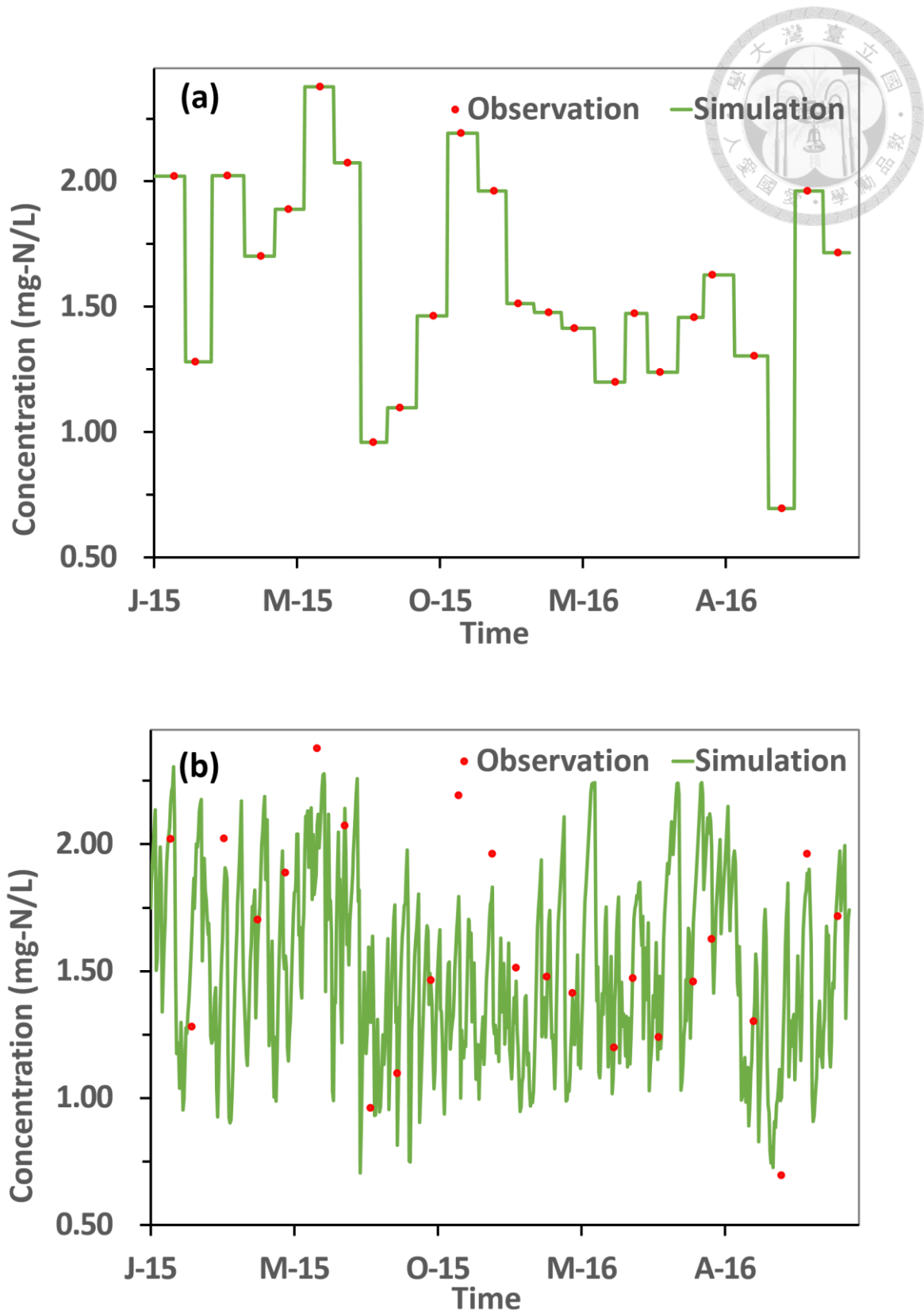


**Figure 2.** The model-fitted  $\text{NO}_3^-$  concentration of site no.1 for an unmeasured time sequence based on (a) a rectangular interpolation and (b) a simple linear regression model using functions in the loadflex package. The red points and green line stand for observations and concentration predictions, respectively.

## 2.6. Variation Partitioning: PCA, RDA and pRDA

To tackle collinearity issues, many researchers have used principal components analysis (PCA) to reduce a number of correlated variables into a set of uncorrelated variables, which reserves its total variance and uncovers its hidden patterns (Varanka et al., 2012). In addition, in order to realize the relative importance of different explanatory variables and their interactive effects, direct gradient analysis such as redundancy analysis (RDA) and its successive partial constrained ordinations, i.e., partial RDA (pRDA) have been commonly proposed (ter Braak, 1998; Borcard et al., 2014). This allows researchers to explore the relationships between predictor variables and dependent variables by removing the intertwined effects among them (Liu, 1997). However, most previous studies utilized PCA or RDA methods focusing on the relationship between biological phenomena and environmental influence, and there are only a few studies on water quality (e.g., Nava-López et al., 2016). Therefore, exploring the likely collinear controlling factors and their internal relationships to riverine DIN transport based on PCA and RDA will be valuable.

In order to interpret the spatial and temporal patterns of riverine  $\text{NO}_3^-$  and  $\text{NH}_4^+$  export and unravel the dependency among controlling factors, i.e., the human disturbance, climatic factors and landscape settings (Table 1), the whole analysis was carried out in three steps (Liu, 1997): (i) the PCA was applied to find out a set of uncorrelated variables, (ii) detailed relations between export and each one of the controlling factors were displayed using a scatterplot matrix, and (iii) the RDA and pRDA were conducted to disentangle the contribution of the major variables.

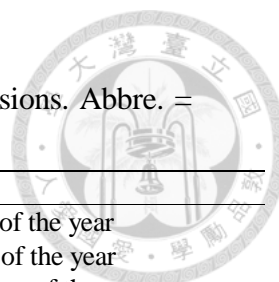
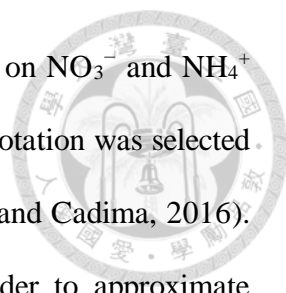


**Table 1.** Definition of different variables used in the three dimensions. Abbre. = abbreviation.

<b>Dimension</b>	<b>Variables</b>	<b>Abbre.</b>	<b>Definition</b>	
Climatic Factors	Rainfall (mm)	RDry RWet	Rainfall in dry season of the year Rainfall in wet season of the year	
	Streamflow (mm)	SFDry SFWet	Discharge rate in dry season of the year Discharge rate in wet season of the year	
	Temperature (°C)	T	The degree of hotness or coldness of environment	
	Channel length (km)	CL	Total length of the stream channel	
Landscape Settings	Longest channel length (km)	LCL	The length of the longest stream channel in watershed	
	Relief	Rel	The difference between the highest and lowest elevations in watershed	
	Area (km <sup>2</sup> )	A	Drainage area of watershed	
	Slope (%)	SLP100	SLP100	The average slope in the 100 m buffer zone
		SLP200	SLP200	The average slope in the 200 m buffer zone
		SLP500	SLP500	The average slope in the 500 m buffer zone
		SLP1000	SLP1000	The average slope in the 1000 m buffer zone
		SLP2000	SLP2000	The average slope in the 2000 m buffer zone
	SLP	SLP	The average slope in watershed	
	Drainage density (km <sup>-1</sup> )	DD	Total channel length over drainage area	
L/G (m)		The ratio of median flow path length to median flow path gradient		
Human Disturbances	Population density (population km <sup>-2</sup> )	PD100	Population density in the 100 m buffer zone	
		PD200	Population density in the 200 m buffer zone	
		PD500	Population density in the 500 m buffer zone	
		PD1000	Population density in the 1000 m buffer zone	
		PD2000	Population density in the 2000 m buffer zone	
		PD	Population density in watershed	
	Buildup (%)	BD100	The percentage of buildup area in the 100 m buffer zone	
		BD200	The percentage of buildup area in the 200 m buffer zone	
		BD500	The percentage of buildup area in the 500 m buffer zone	
		BD1000	The percentage of buildup area in the 1000 m buffer zone	
		BD2000	The percentage of buildup area in the 2000 m buffer zone	
	BD	The percentage of the buildup area in watershed		
	Agriculture (%)	AGR100	The percentage of agriculture in the 100 m buffer zone	
		AGR200	The percentage of agriculture in the 200 m buffer zone	
		AGR500	The percentage of agriculture in the 500 m buffer zone	
AGR1000		The percentage of agriculture in the 1000 m buffer zone		
AGR2000		The percentage of agriculture in the 2000 m buffer zone		
AGR	The percentage of the agriculture in the watershed			

PCA was applied to reduce redundant information and to transform the original correlated data into another set of uncorrelated variables. The PCA keeps only a few independent sets (patterns) of environmental data that are distinct from each other, which



will help to realize the effects of various characteristics of watersheds on  $\text{NO}_3^-$  and  $\text{NH}_4^+$  exports in our study (Liu, 1997; Johnson et al., 2007). The varimax rotation was selected to better separate divergent groups of variables, as suggested (Jolliffe and Cadima, 2016). The environmental variables were centered and standardized in order to approximate normally distributed random errors and then were derived from the PCs via a standardized linear projection which maximizes the variance in the projected space (Hotelling, 1933). For a set of observed-dimensional data vectors,  $\{t_n\}$ ,  $n \in \{1, \dots, N\}$ , the  $q$  principal axes  $\{w_j\}$ ,  $j \in \{1, \dots, q\}$ , could be derived as the orthonormal axes onto which the retained variance under projection is maximal. It can be shown that the vectors  $w_j$  are given by the  $q$  dominant eigenvectors (i.e., those with the largest associated eigenvalues  $\lambda_j$ ) of the sample covariance matrix. The outcomes of PCA help us to identify relationships between these variables and determine which variables require further investigation. The variables with loading higher than 0.1 in the first and second PCs were kept for the following RDA and pRDA analysis to constrain the ordination of environmental variables and to avoid the collinearity problem (Sutter and Kalivas, 1993; Johnson et al., 2007).

Moreover, we know water quality is regulated by riparian zones along the river and stream networks, but what needs to be clarified is spatially to what extent their individual effect is (Uriarte et al., 2011). Here, we delineated the buffer zones of 100, 200, 500, 1000 and 2000 m along the stream network using the buffer tool in ArcGIS v.10.7. (ESRI Inc., Redlands, CA, USA) The environmental variables within the entire watershed and five buffer zones were also retrieved as previous studies suggested (Nielsen et al., 2012; Nava-López et al., 2016; Xiao et al., 2016). The land cover/land use data were acquired from the Ministry of the Interior of Taiwan (Figure 1b; <https://www.moi.gov.tw>), and the digital elevation model (DEM) data were derived from the open data platform in Taiwan

(<https://data.gov.tw/>), which were provided as input for calculations of landscape settings and human disturbance variables (Table 1).

The RDA and pRDA were further applied to quantify the individual effect and integrative contribution among human disturbance, climatic factors and landscape setting on riverine  $\text{NO}_3^-$  and  $\text{NH}_4^+$  exports (ter Braak 1988). RDA extends the algorithm of PCA with a response matrix  $Y$  (with  $n$  objects and  $p$  variables) by an explanatory matrix  $X$  (with  $n$  objects and  $m$  variables). First, RDA produces a matrix of fitted values  $\hat{Y}$  through Equation (2),

$$\hat{Y} = X[X'X]^{-1}X'Y, \quad (2)$$

and second, runs a PCA based on  $\hat{Y}$  (Legendre and Legendre, 2012).

For pRDA, the additional explanatory variables, called covariables, are assembled in matrix  $W$ ; the linear effects of the explanatory variables in  $X$  on the response variables in  $Y$  are adjusted for the effects of the covariables in  $W$  (Legendre et al., 2011). In our study, the total variance of riverine  $\text{NO}_3^-$  and  $\text{NH}_4^+$  exports could be explained by the variables derived from human disturbance, climatic factors and landscape setting, and their individual contribution of  $\text{NO}_3^-$  and  $\text{NH}_4^+$  export can be finally figured out. We further partitioned the total variation of the riverine  $\text{NO}_3^-$  and  $\text{NH}_4^+$  response variables using three steps (Table 2). First, canonical ordination with no covariables was used to estimate the total amount of variance explained (as sum of canonical eigenvalues) in the  $\text{NO}_3^-$  and  $\text{NH}_4^+$  export attributed to all explanatory variables, human disturbances (H), climatic factors (C) and landscape setting (L), and the total unexplained variance (1-HCL). Second, the combinations of various covariables were considered to calculate the separate effect of each variable (H, C or L), in which an individual predictor variable was run (e.g., H) with the remaining other two as covariables (e.g., C&L). Third, a series of partial canonical ordinations were used to calculate the unique and interactive effects for each set of

predictors (e.g., C&L–H) by considering the interaction term of interest as explanatory (C&L) and excluding the effect of not interest (e.g., H). For more details of calculations, please refer to Borcard et al. (1992) and Liu (1997).

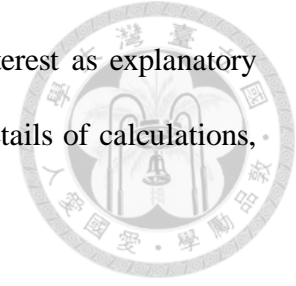


**Table 2.** Eigenvalues of partial RDA (pRDA) of  $\text{NO}_3^-$  and  $\text{NH}_4^+$  and separate climatic (C), landscape setting (L) and human disturbance (H) and interactive effects among C, L and H.

Environmental factor	Covariable	$\lambda\text{NO}_3^-$		$\lambda\text{NH}_4^+$	
		Wet	Dry	Wet	Dry
Unexplained variable		0.27	0.14	0.31	0.21
CLH	None	0.73	0.86	0.69	0.79
C	L&H	0.31	0.27	0.03	0.02
L&H	C	0.44	0.27	0.68	0.77
L	C&H	0.00	0.00	0.05	0.00
C&H	L	0.41	0.74	0.06	0.18
H	C&L	0.07	0.09	0.02	0.13
C&L	H	0.31	0.2	0.08	0.02



### 3. Results

#### 3.1. Riverine DIN Concentration and Export

The mean DIN concentration is  $1.66 \text{ mg-N L}^{-1}$ , ranging from  $0.28$  to  $8.91 \text{ mg-N L}^{-1}$ , while the mean  $\text{NO}_3^-$  concentration is  $0.98 \text{ mg-N L}^{-1}$ , varying from  $0.26$  to  $2.79 \text{ mg-N L}^{-1}$ , and the mean  $\text{NH}_4^+$  concentration is  $0.56 \text{ mg-N L}^{-1}$ , in the range of  $0.01$ – $4.59 \text{ mg-N L}^{-1}$ . Generally, the mean  $\text{NO}_3^-$  concentration is higher in the wet season ( $1.03 \text{ mg-N L}^{-1}$ ) than in the dry season ( $0.79 \text{ mg-N L}^{-1}$ ). In contrast, the mean DIN and  $\text{NH}_4^+$  concentrations have higher values in the dry season ( $1.82$  and  $0.95 \text{ mg-N L}^{-1}$ ) than in the wet season ( $1.66$  and  $0.48 \text{ mg-N L}^{-1}$ ) (Tables 3, S2 and S3). The annual mean DIN export of 43 watersheds island-wide is  $3100 \text{ kg-N km}^{-2} \text{ yr}^{-1}$ , ranging from  $230$  to  $10,000 \text{ kg-N km}^{-2} \text{ yr}^{-1}$  (Figure 3 and Table 3), in which the highest DIN export (site 16) reaches over 40-fold of the lowest one (site 39; Tables S4 and S5). Generally, watersheds with high DIN,  $\text{NO}_3^-$  and  $\text{NH}_4^+$  concentrations/exports locate in northern and southwestern Taiwan, while watersheds with relatively low DIN,  $\text{NO}_3^-$  and  $\text{NH}_4^+$  concentrations/exports are those in central and eastern Taiwan. However, high  $\text{NO}_3^-$  export does not always correspond to high  $\text{NH}_4^+$  export (e.g., site 41) (Figure 3, Tables S4 and S5). Meanwhile, DIN exports present a significant seasonality that the wet season (from May to October) can contribute over 75% of the annual export on average, and the  $\text{NO}_3^-$  and  $\text{NH}_4^+$  exports during wet and dry seasons also account for 70–80% and 20–30% of annual DIN exports respectively (Tables S4 and S5). However, the contributions of  $\text{NO}_3^-$  and  $\text{NH}_4^+$  for wet and dry seasons to annual DIN export varied among watersheds. For example, the lowest DIN export is  $227 \text{ kg-N km}^{-2} \text{ yr}^{-1}$  in site 39, a relatively pristine watershed (87% of forest cover), and the contributions of  $\text{NO}_3^-$  and  $\text{NH}_4^+$  exports in the wet (dry) season to annual DIN export are both 90% (10%). In contrast, the highest DIN export,  $10,228 \text{ kg-N km}^{-2} \text{ yr}^{-1}$ , appears in site 16, a

more disturbed watershed (65% of agricultural land cover), and the contributions of the  $\text{NO}_3^-$  and  $\text{NH}_4^+$  exports in the wet (dry) season to annual DIN export are 85% (15%) and 55% (45%) (Tables S4 and S5).

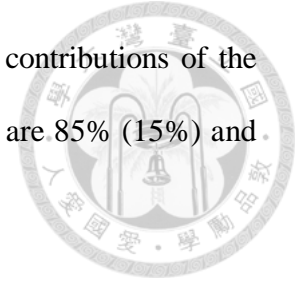


**Table 3.** Mean estimated seasonal  $\text{NO}_3^-$ ,  $\text{NH}_4^+$  and dissolved inorganic nitrogen (DIN) concentrations and exports for 43 sampling sites in the study period (unit:  $\text{mg-N L}^{-1}$  for conc. and  $\text{kg-N km}^{-2} \text{yr}^{-1}$  for flux).

	Annual		Dry Season		Wet Season	
	Conc.	Flux	Conc.	Flux	Conc.	Flux
$\text{NO}_3^-$						
Mean	0.98	1936	0.79	429	1.03	1507
( $\pm$ SD)	( $\pm$ 0.59)	( $\pm$ 1363)	( $\pm$ 0.51)	( $\pm$ 520)	( $\pm$ 0.66)	( $\pm$ 1085)
Min–Max	0.26–2.79	212–5801	0.14–2.19	7–2917	0.25–3.58	158–4908
$\text{NH}_4^+$						
Mean	0.56	977	0.95	333	0.48	644 ( $\pm$ 950)
( $\pm$ SD)	( $\pm$ 0.96)	( $\pm$ 1456)	( $\pm$ 1.73)	( $\pm$ 551)	( $\pm$ 0.81)	
Min–Max	0.01–4.59	9–5757	0.01–9.13	1–2372	0.01–3.81	7–3942
DIN						
Mean	1.66	3100	1.82	798	1.66	2303
( $\pm$ SD)	( $\pm$ 1.69)	( $\pm$ 2827)	( $\pm$ 2.07)	( $\pm$ 982)	( $\pm$ 1.74)	( $\pm$ 2041)
Min–Max	0.28–8.91	227–10229	0.16–9.74	8–4730	0.28–10.45	185–7527

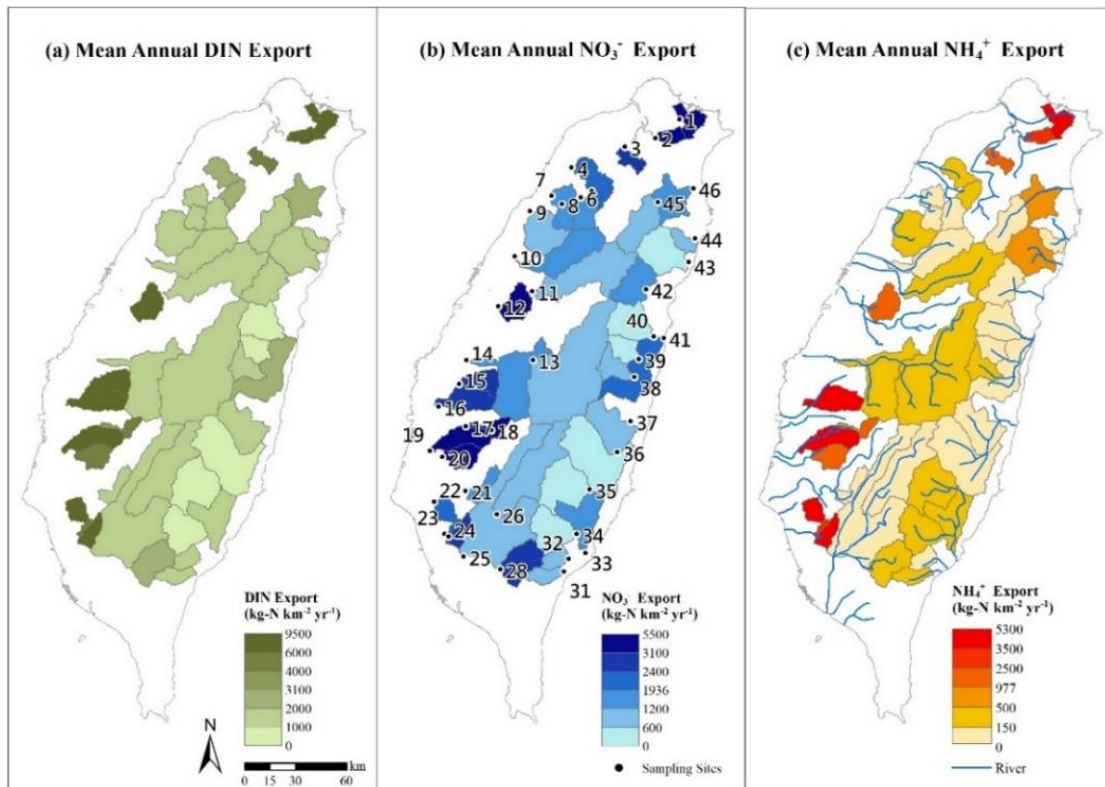


**Figure 3.** The spatial patterns of DIN (a),  $\text{NO}_3^-$  (b) and  $\text{NH}_4^+$  (c) exports of 43 watersheds. The numbers in panel (b) indicate the sampling sites.



The compositions of  $\text{NO}_3^-$  and  $\text{NH}_4^+$  between pristine and disturbed watershed (forest cover <50%) varied as well. For instance, in relatively pristine watersheds, such as site 38 (Figure 4a),  $\text{NO}_3^-$  exports were generally higher (~70%) than  $\text{NH}_4^+$  (~20%). On the contrary,  $\text{NH}_4^+$  exports can reach 40% of annual DIN in the higher disturbed watersheds with a smaller drainage area (<1000 km<sup>2</sup>) and steep slopes (>30%), such as site 1 (Figure 4b). In addition, some watersheds with higher  $\text{NH}_4^+$  exports in lieu of  $\text{NO}_3^-$  are scattered in the plain (slope <20%) in southwestern Taiwan, such as sites 15, 16 and 22 (Figure 3, Tables S4 and S5).

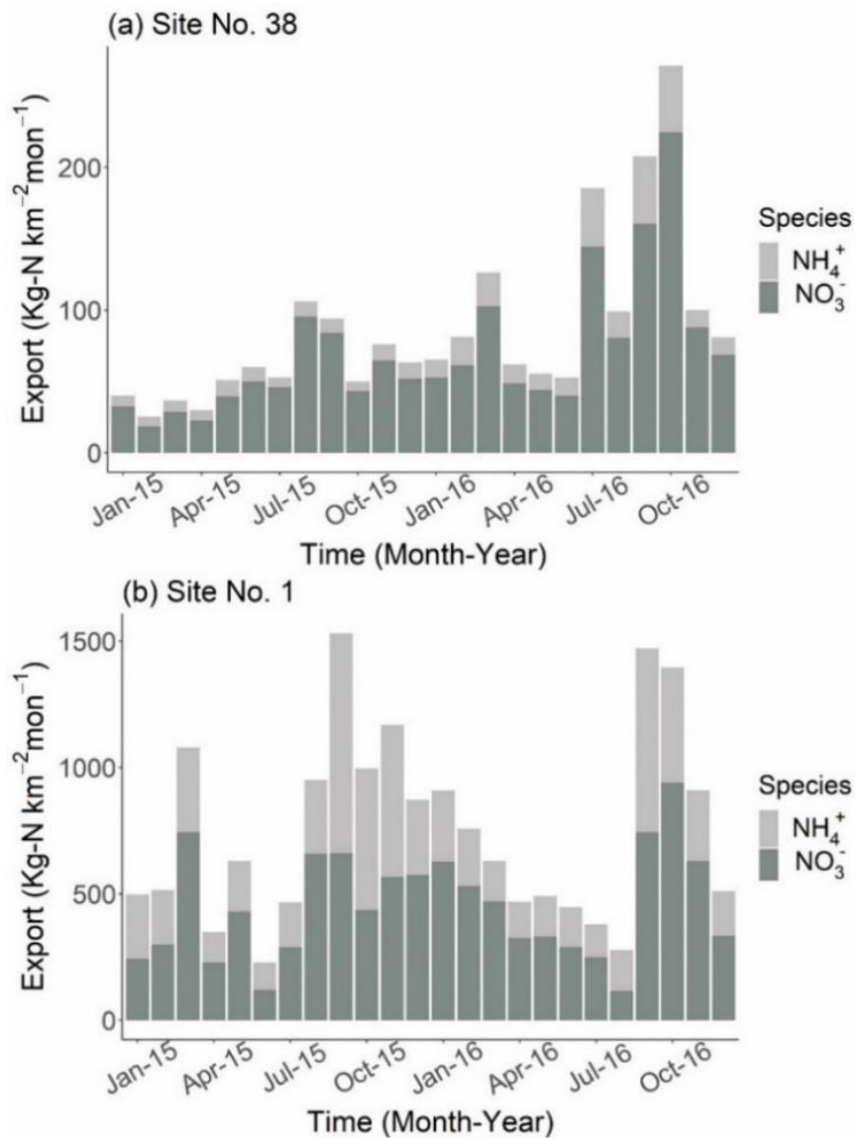
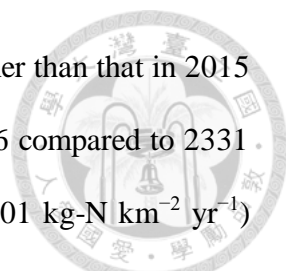


**Figure 4.** The monthly  $\text{NO}_3^-$  and  $\text{NH}_4^+$  exports in site no. 38 (a) and no. 1 (b) during the study period.



The average DIN export in 2016 ( $3460 \text{ kg-N km}^{-2} \text{ yr}^{-1}$ ) was higher than that in 2015 ( $2723 \text{ kg-N km}^{-2} \text{ yr}^{-1}$ ) due to much higher rainfall, 3480 mm in 2016 compared to 2331 mm in 2015 (Tables S4 and S5). The mean  $\text{NO}_3^-$  export in 2016 ( $2301 \text{ kg-N km}^{-2} \text{ yr}^{-1}$ ) was higher than in 2015 ( $1553 \text{ kg-N km}^{-2} \text{ yr}^{-1}$ ), whereas the mean  $\text{NH}_4^+$  export in 2016 ( $940 \text{ kg-N km}^{-2} \text{ yr}^{-1}$ ) was slightly lower than 2015 ( $1016 \text{ kg-N km}^{-2} \text{ yr}^{-1}$ ), in which most of the decreased  $\text{NH}_4^+$  exports appeared in watersheds in northern Taiwan, while some  $\text{NH}_4^+$  exports increased in watersheds in southern and eastern Taiwan (Tables S4 and S5).

### 3.2. Scatterplot Matrix

The correlations between nutrient exports and variables at different buffer zones show that significantly higher coefficients are generally found between annual and seasonal nutrient exports and variables at watershed scale (Figures S1–S3), whereas the fraction of buildup area within a 100 m buffer has higher correlations to DIN ( $r = 0.82$ ,  $p < 0.01$ ) in the dry season than other variables among different buffer zones (Figure S3). Streamflow, the fraction of agricultural land cover of the entire watershed, buildup area within a 100 m buffer zone and buildup area of the entire watershed show significant positive relationships to DIN export ( $r = 0.52 - 0.64$ ,  $p < 0.01$ ; Figure 5). However, there is a negative relationship found between DIN and slope of entire watershed ( $r = -0.64$ ,  $p < 0.01$ ; Figure 5).

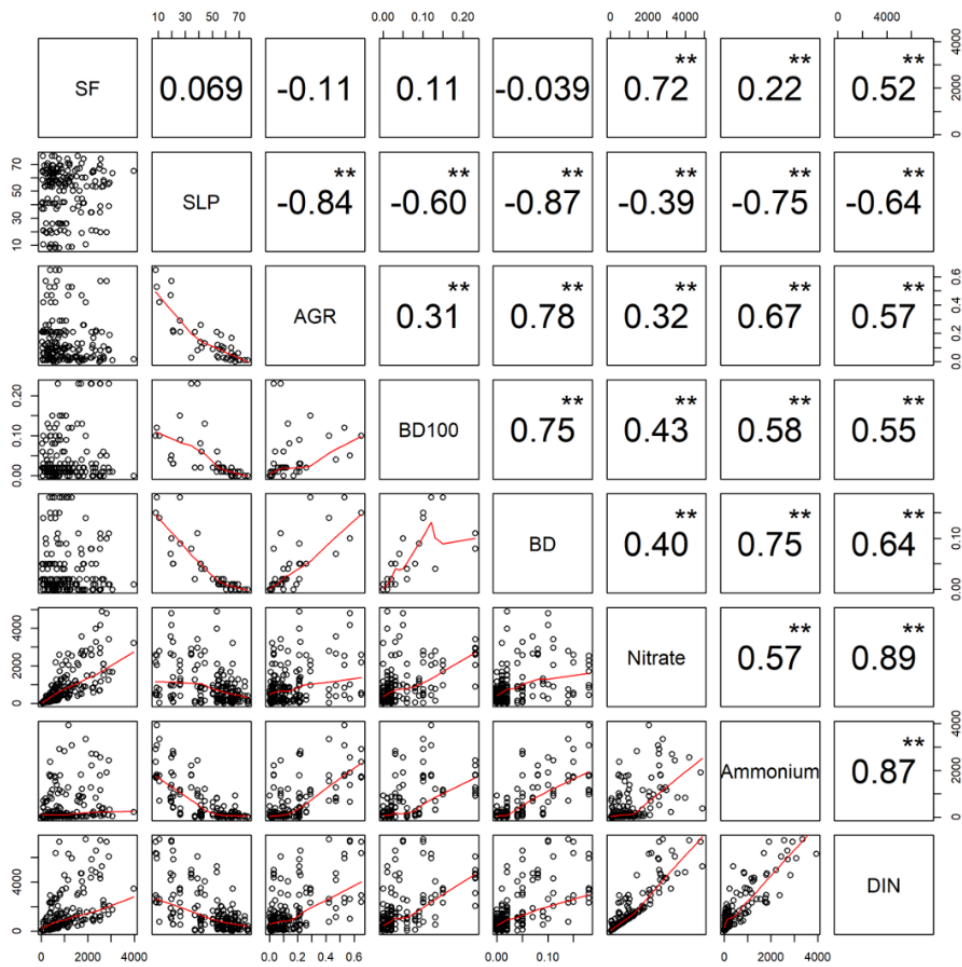
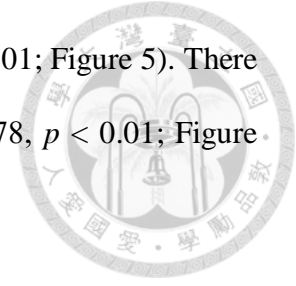


**Figure 5.** Scatterplot matrix among relative streamflow [SF; mm], slope at watershed scale [SLP; %], the proportion of agriculture at watershed scale [AGR; %], the proportion of buildup in 100 m buffer zone [BD100; %], the proportion of buildup at watershed scale [BD; %],  $\text{NO}_3^-$ ,  $\text{NH}_4^+$ , and DIN exports based on all sampling sites. The asterisk indicates that the correlation is statistically significant ( $p$ -value: \*\* < 0.01 < \* < 0.05), and the red lines indicate smooth transition regressions.

Streamflow positively correlates to  $\text{NO}_3^-$  ( $r = 0.72$ ,  $p < 0.01$ ) and  $\text{NH}_4^+$  ( $r = 0.22$ ,  $p < 0.01$ ; Figure 5). The exports of the two ions also significantly correlate to agriculture, buildup area in a 100 m buffer zone and buildup area within the entire watershed, of which the correlation coefficients are higher in  $\text{NH}_4^+$  ( $r = 0.58 - 0.75$ ,  $p < 0.01$ ; Figure 5) than in  $\text{NO}_3^-$  ( $r = 0.32 - 0.43$ ,  $p < 0.01$ ; Figure 5). However, the slope is negatively significantly related to  $\text{NO}_3^-$  exports ( $r = -0.39$ ,  $p < 0.01$ ),  $\text{NH}_4^+$  exports ( $r = -0.75$ ,  $p < 0.01$ ), agriculture ( $r = -0.84$ ,  $p < 0.01$ ), buildup area within the 100 m buffer zone ( $r = -0.60$ ,  $p < 0.01$ ), and buildup area within the entire watershed ( $r = -0.87$ ,  $p < 0.01$ ).

< 0.01) and buildup area within the entire watershed ( $r = -0.87$ ,  $p < 0.01$ ; Figure 5). There are positive correlations among variables of landcover ( $r = 0.31 - 0.78$ ,  $p < 0.01$ ; Figure 5).



### 3.3. PCA of Environmental Variables

The first two principal components with eigenvalues  $> 5.0$  are retained, accounting for 70.6% and 72.5% of variances on  $\text{NO}_3^-$  and  $\text{NH}_4^+$  exports, respectively (Figure 6). The combinations of variables within the watershed scale (SF, SLP, AGR, and BD) and buildup area in a 100 m buffer (BD100) can explain much more variances of  $\text{NO}_3^-$  and  $\text{NH}_4^+$  exports than the performance using variables derived from the separate buffer zones ( $\leq 60\%$ ; Figure S4). Generally, the spatial variability of buildup (BD) and slope (SLP) are the main ingredients of the first PCs for  $\text{NO}_3^-$  and  $\text{NH}_4^+$  (Figure 6). The second PC is associated with seasonal variables, i.e., streamflow (SF<sub>Wet</sub> and SF<sub>Dry</sub>) and rainfall (RW<sub>Wet</sub> and RW<sub>Dry</sub>) during wet and dry periods. Most environmental variables displayed positive correlations with these two response variables ( $\text{NO}_3^-$  and  $\text{NH}_4^+$ ), except for landscape setting variables such as area (A), channel length (CL), longest channel length (LCL), relief (R) and slope (SLP), i.e., the opposite direction to  $\text{NO}_3^-$  and  $\text{NH}_4^+$  export (blue lines in Figure 6). During the wet season, the smaller projected angle is between the fraction of BD and  $\text{NO}_3^-$  export (Ni<sub>Wet</sub>), indicating high relevance between human impact and the wet season  $\text{NO}_3^-$  export, while during the dry season,  $\text{NO}_3^-$  export relates to the vectors dominated by streamflow and rainfall. However, unlike  $\text{NO}_3^-$  export,  $\text{NH}_4^+$  export is dominated by BD regardless of the different seasons. According to the results derived from PCA, five environmental variables including streamflow, slope, the fraction of agricultural land cover, buildup area within a 100 m buffer zone and buildup area of the entire watershed with higher loading were selected for further analysis.

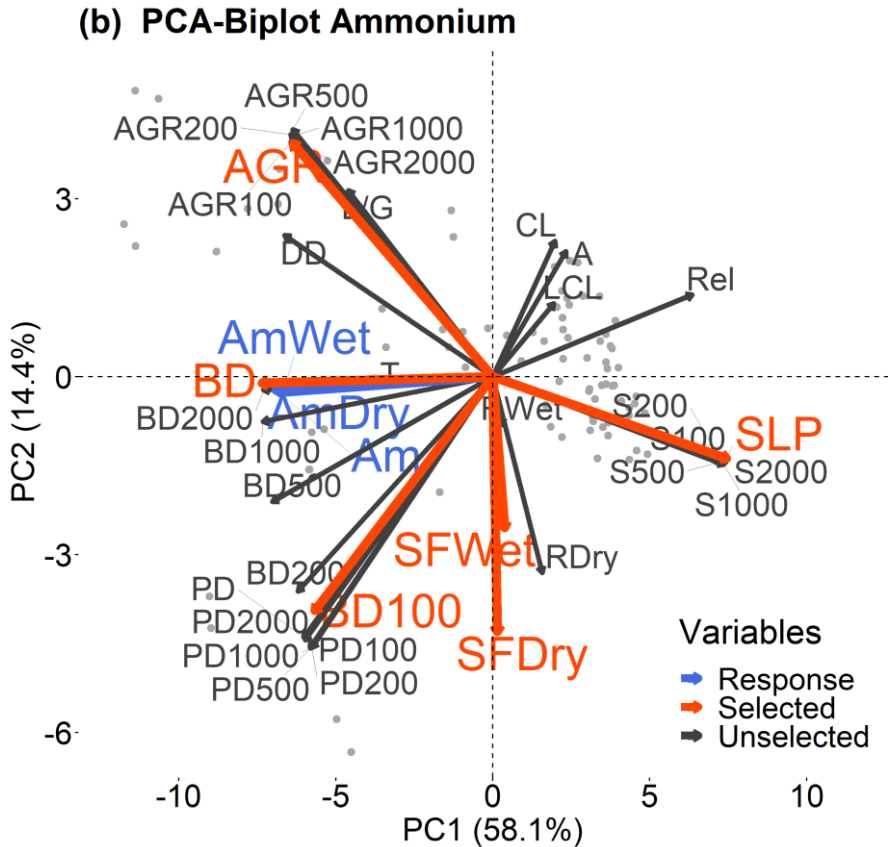
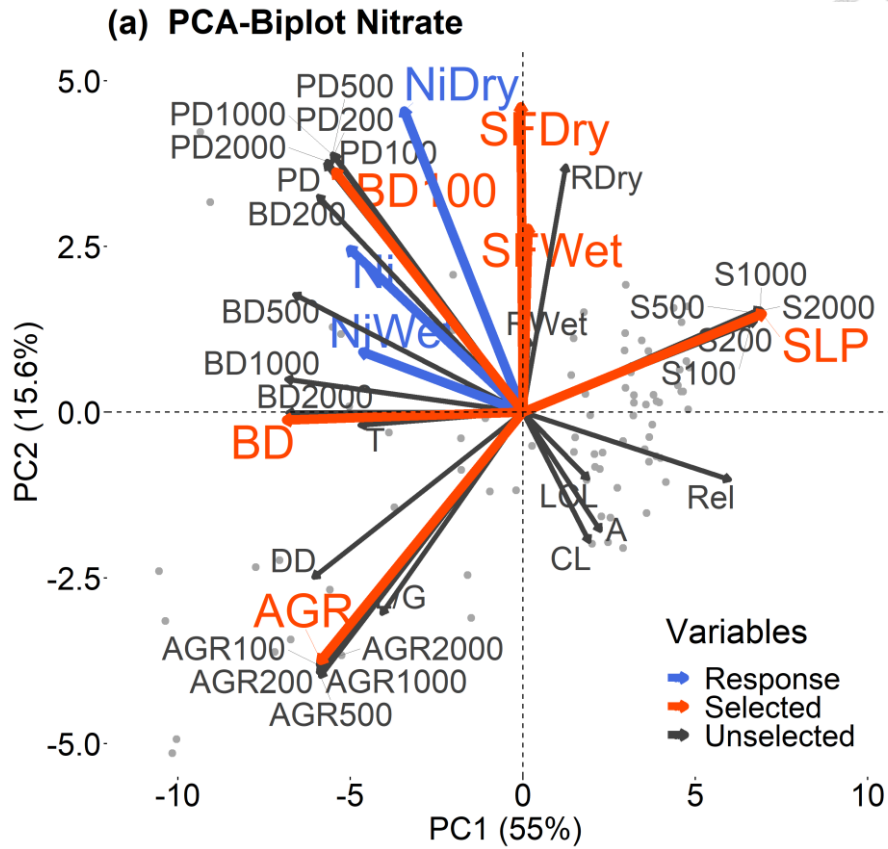
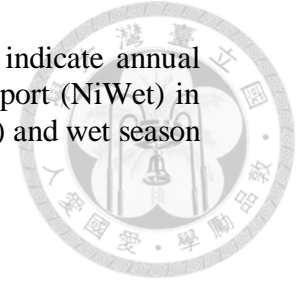


**Figure 6.** Principal components analysis of environmental variables for 43 catchments (gray dots) for  $\text{NO}_3^-$  (a) and  $\text{NH}_4^+$  export (b). Red-labeled variables

are main components for PC1 and PC2. Blue-labeled variables indicate annual nitrate (Ni), dry season nitrate (NiDry) and wet season nitrate export (NiWet) in (a) and annual ammonium (Am), dry season ammonium (AmDry) and wet season ammonium export (AmWet) in (b).



### 3.4. Variance Partitioning—RDA and pRDA

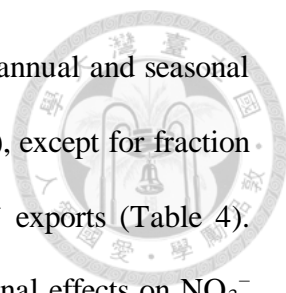
The RDA model shows that the total variance explained (total inertia) by five selected environmental variables is always higher on  $\text{NO}_3^-$  exports than on  $\text{NH}_4^+$  exports. These predictor variables can explain 86% and 79% of the total variance of  $\text{NO}_3^-$  and  $\text{NH}_4^+$  exports, respectively, in the dry season, but only 73% and 69% in the wet season (Table 4).

**Table 4.** The marginal effects ( $\lambda_1$ ) and total inertia (total effects) of climatic, landscape setting and human disturbance variables on  $\text{NO}_3^-$  and  $\text{NH}_4^+$  exports based on 43 sampling sites.

Species	$\text{NO}_3^-$			$\text{NH}_4^+$		
	Annual	Wet	Dry	Annual	Wet	Dry
	$\lambda_1$	$\lambda_1$	$\lambda_1$	$\lambda_1$	$\lambda_1$	$\lambda_1$
Climatic						
Streamflow (mm)	0.52**	0.28**	0.59**	0.05**	0.01 <sup>ns</sup>	0.02 <sup>ns</sup>
Landscape setting						
Slope (%)	0.15**	0.32**	0.12**	0.56**	0.64**	0.61**
Human disturbance						
Agri. (%)	0.11**	0.31**	0.01 <sup>ns</sup>	0.44**	0.47**	0.53**
Buildup_100 m (%)	0.18**	0.19**	0.57**	0.33**	0.32**	0.46**
Buildup (%)	0.16**	0.26**	0.21**	0.57**	0.58**	0.73**
Total inertial	0.74	0.73	0.86	0.68	0.69	0.79

\* $p < 0.05$ ; \*\* $p < 0.01$ . ns: not significant.

Streamflow reveals the highest marginal effects on  $\text{NO}_3^-$  exports, where marginal effects  $\lambda_1$  increase from 0.28 in the wet season, 0.52 in annual export, to 0.59 in the dry season. However, the effects of streamflow are low ( $\lambda_1 < 0.05$ ) for  $\text{NH}_4^+$  annual and seasonal exports (Table 4). In contrast, slope has lower marginal effects on annual and seasonal  $\text{NO}_3^-$  exports ( $\lambda_1 = 0.12 - 0.32$ ) than on  $\text{NH}_4^+$  exports ( $\lambda_1 = 0.56 - 0.64$ ), and the marginal effects of slope are higher in the wet season ( $\lambda_1 = 0.32 - 0.64$ ) than in the dry season ( $\lambda_1 = 0.12 - 0.61$ ) for nutrient export (Table 4). The anthropogenic factors, including the fraction of agricultural land cover, buildup area within a 100 m buffer and



buildup area of the entire watershed, show higher marginal effects on annual and seasonal  $\text{NH}_4^+$  exports ( $\lambda_1 = 0.32 - 0.73$ ) than  $\text{NO}_3^-$  exports ( $\lambda_1 = 0.01 - 0.57$ ), except for fraction of buildup area within a 100 m buffer in the dry season on  $\text{NO}_3^-$  exports (Table 4). Generally, buildup area within a 100 m buffer zone has higher marginal effects on  $\text{NO}_3^-$  exports ( $\lambda_1 = 0.18 - 0.57$ ) than buildup area of entire watershed ( $\lambda_1 = 0.16 - 0.26$ ), although the effect of buildup area within a 100 m buffer is slightly lower ( $\lambda_1 = 0.19$ ) than buildup area of entire watershed ( $\lambda_1 = 0.26$ ) in the wet season. In the dry season, the effect of buildup area within a 100 m buffer is 2.5 times ( $\lambda_1 = 0.57$ ) that of buildup area of entire watershed ( $\lambda_1 = 0.21$ ). For  $\text{NH}_4^+$  exports, buildup area of entire watershed has the highest effects ( $\lambda_1 = 0.57 - 0.73$ ) compared with agriculture ( $\lambda_1 = 0.44 - 0.53$ ) and buildup area within a 100 m buffer ( $\lambda_1 = 0.32 - 0.46$ ; Table 4).

For  $\text{NO}_3^-$  exports in pRDA, the lowest (highest) eigenvalue of pure effect on a single variable included is the landscape (climatic) variable in the wet season, 0.003 (0.31), and in the dry season, 0.004 (0.27) (Figure 7). The climatic variable (C) seems to be the dominant factor regarding seasonal  $\text{NO}_3^-$  exports. It is responsible for over 42% and 31% of variance for wet and dry seasonal  $\text{NO}_3^-$  exports (Figure 7). The combination of landscape with human disturbance variables (LH) will contribute a significant effect on  $\text{NO}_3^-$  export in the wet season (0.38 of eigenvalue and 51.59% of explained variance), but decreases substantially in the dry season (0.17 of eigenvalue and 20.00% of explained variance) (Figure 7). While the effects of the combination of climatic with human disturbance variables (CH) increase from 0.04 (5.32% of explained variance) in the wet season (Figure 7a) to 0.38 (44.15% of explained variance) in the dry season (Figure 7b).

For  $\text{NH}_4^+$  exports in pRDA, the eigenvalues of each single variable (pure effect) are lower than 0.05 (Figure 8). The only exception is the pure effect on human disturbance variables in the dry season ( $H = 0.13$ ), which accounts for 16.4% of explained variance

(Figure 8). The dominant effect is the combination of landscape with human disturbance variables (LH) in which eigenvalues reach 0.61 (88.5%) and 0.64 (80.7%) of the total  $\text{NH}_4^+$  export variance in the wet and dry season, respectively (Figure 8). Other interactive effects are much lower than LH in both seasons.

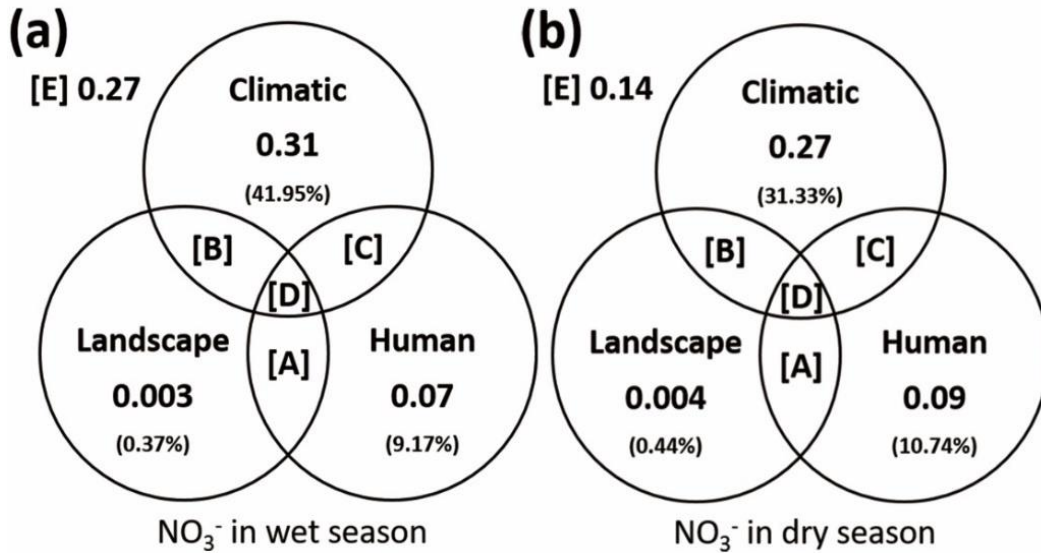


**Figure 7.** Variance decomposition (conditional effects) of  $\text{NO}_3^-$  exports in wet (a) and dry (b) seasons in 43 watersheds. Each circle and the intersections indicate the individual effect of climatic [C], landscape (L) and human disturbance (H) variables and their interactive effects on  $\text{NO}_3^-$  export from pRDA, including the shared variance of landscape setting and human disturbance (LH) [A], landscape setting and climatic variables (LC) [B], climatic variables and human disturbance (CH) [C], among three variables (CLH) [D], and residual variance [E]. In Panel (a): [A] = 0.38 (51.59%); [B] = -0.002 (-0.29%); [C] = 0.04 (5.32%); [D] = -0.06 (-8.09%). In Panel (b): [A] = 0.17 (20.00%); [B] = -0.004 (-0.43%); [C] = 0.38 (44.15%); [D] = -0.05 (-6.22%). The percentage of explained variation of variables is equal to the eigenvalue divided by total inertia.



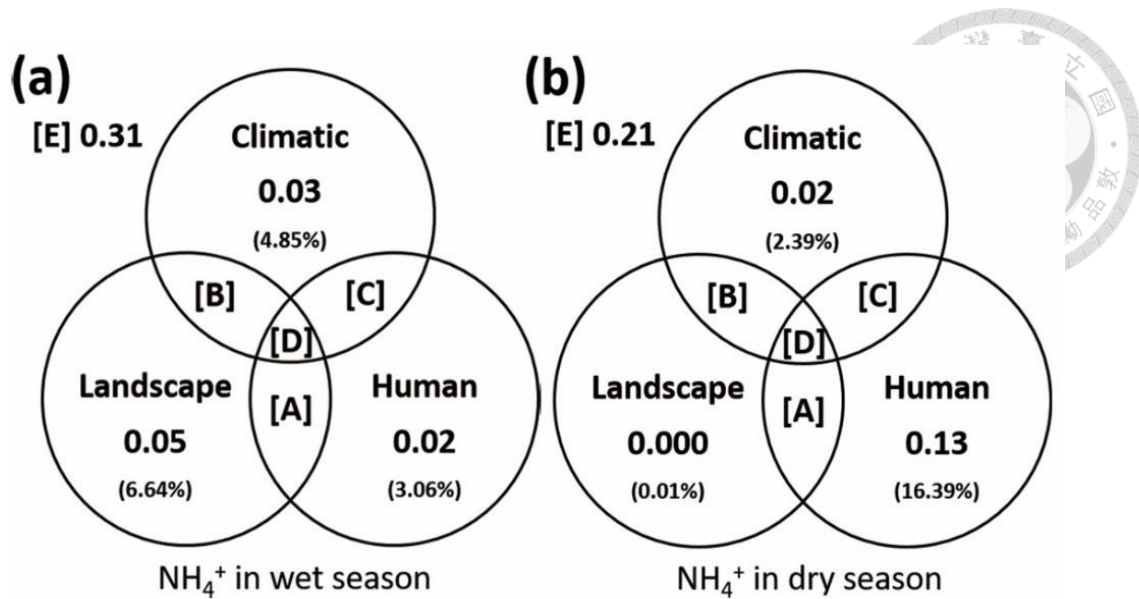


**Figure 8.** Variance decomposition (conditional effects) of  $\text{NH}_4^+$  exports in wet (a) and dry (b) seasons in 43 watersheds. Each circle and the intersections indicate the individual effect of climatic [C], landscape (L) and human disturbance (H) variables and their interactive effects on  $\text{NH}_4^+$  export from pRDA, including the shared variance of landscape setting and human disturbance (LH) [A], landscape setting and climatic variables (LC) [B], climatic variables and human disturbance (CH) [C], among three variables (CLH) [D], and residual variance [E]. In Panel (a): [A] = 0.61 (88.54%); [B] = -0.004 (-0.56%); [C] = 0.001 (0.09%); [D] = -0.02 (-2.62%). In Panel (b): [A] = 0.64 (80.70%); [B] = 0.001 (0.08%); [C] = 0.03 (4.10%); [D] = -0.03 (-3.67%). The percentage of explained variation of variables is equal to the eigenvalue divided by total inertia.

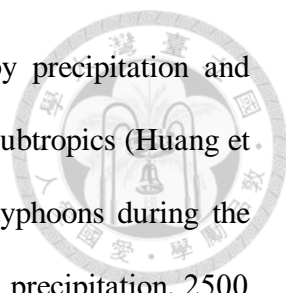
## 4. Discussion



### 4.1. Characteristics of DIN Concentrations and Exports in Taiwan

On average, DIN concentration from 43 island-wide watersheds across Taiwan is 1.66 mg-N L<sup>-1</sup>, and the two main DIN species present a mediated dilution effect with streamflow (Table 3 and Figure S5). The average riverine DIN export reaches 3100 kg-N km<sup>-2</sup> yr<sup>-1</sup>, which is much greater than the global mean (208 kg-N km<sup>-2</sup> yr<sup>-1</sup>) (Huang et al., 2016). High rainfall and streamflow, N deposition and N fertilizer application for agricultural production at upstream regions can account for the significant nutrients streamflow (Huang et al., 2012). The results reveal that DIN export and concentration vary spatially, ranging from 200 kg-N km<sup>-2</sup> yr<sup>-1</sup>, 0.3 mg-N L<sup>-1</sup> in less disturbed watersheds (site 39; Figure 3), to over 10,000 kg-N km<sup>-2</sup> yr<sup>-1</sup>, 8.8 mg-N L<sup>-1</sup> in highly disturbed watersheds (site 16; Figure 3). The spatial DIN surge also indicates that the environmental background actually exports DIN and consequently induces the risk of eutrophication in the downstream. Previous studies suggested that intact forested watersheds demonstrated high N retention capacity but the capacity would collapse with significant land cover conversion (Howarth, 1998; Groffman et al., 2004). In our study, higher NH<sub>4</sub><sup>+</sup> exports in highly disturbed watersheds with smaller drainage area (<1000 km<sup>2</sup>) and steep slope (>30%) show that these environmental backgrounds are unfavorable to ammonia oxidation or assimilation due to rapid transport (Halbfaß et al., 2010). In addition, most of the watersheds with higher NH<sub>4</sub><sup>+</sup> exports than NO<sub>3</sub><sup>-</sup> appear in plain areas where human disturbances are high and sewage systems are deficient (Lee et al., 2014).

The island-wide DIN estimation reveals that the wet season (May to October) contributes 78% of the annual DIN export, 3100 kg-N km<sup>-2</sup> yr<sup>-1</sup>, which is consistent with previous findings that hydrological processes control DIN export (Ohowa et al., 1997; He



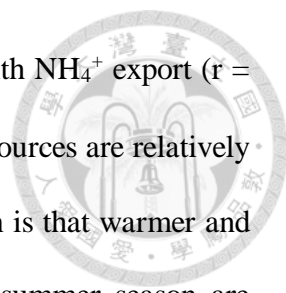
et al., 2011). Because nutrient export and transport is regulated by precipitation and streamflow, this controlling factor is more dominant in the tropics and subtropics (Huang et al., 2016; Chang et al., 2017). The torrential rainfall brought by typhoons during the humid growing summer in Taiwan accounts for 30–50% of the annual precipitation, 2500 mm yr<sup>-1</sup> (Chang et al., 2013; Lee et al., 2013), and consequently causes vital effects on biogeochemical processes, i.e., a huge amount of nutrients being flushed out from terrestrial ecosystems to aquatic ecosystems. It also explains why the nutrient streamflow in Taiwan is in the leading place worldwide (Huang et al., 2016).

#### *4.2. Influences of Main Variables and Their Interactive Effects on DIN Export*

##### *4.2.1. Climatic Control*

In tropical/subtropical mountainous Taiwan, abundant rainfall usually leads to a great amount of net nutrient exports even during the growing summer, which is distinct from the findings in temperate forest ecosystems (Huang et al., 2012; Likens, 2013; Chang et al., 2017). Water is the conveyor of ion movement. In spite of the dilution of NO<sub>3</sub><sup>-</sup> concentration during flood periods (wet season), the extensive runoff by typhoons flushes over surface and near-surface and leads to greater DIN exports (Lee et al., 2013).

The relation between export and streamflow (F-Q relation), which definitely shows export change with streamflow, is particularly crucial as regarding nutrient balance and transport, although the F-Q relation, which inevitably incorporates streamflow in the calculation, could likely lead to the “spurious relation”. However, the F-Q relation, which can present the dominance of supply-limited or kinetically-limited under different hydrologic conditions, helps to indicate the nutrient budget balance, and the transported amount is also important. Notably, there are totally different hydrological controls on NO<sub>3</sub><sup>-</sup> and NH<sub>4</sub><sup>+</sup> transport. One is that streamflow plays a strong role on NO<sub>3</sub><sup>-</sup> export ( $r = 0.72$ ;

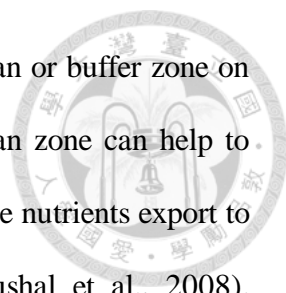


$\lambda_1 = 0.28 - 0.59$ ), which is in contrast to a relatively weak relation with  $\text{NH}_4^+$  export ( $r = 0.22$ ;  $\lambda_1 < 0.05$ ). The positive  $\text{NO}_3^-$  streamflow relation indicates the sources are relatively sufficient, as compared to kinetic transport. One possible interpretation is that warmer and more humid conditions (e.g., higher soil moisture) during the wet summer season are favorable for nitrification and promotes  $\text{NO}_3^-$  accumulation and then transports it from the soil to the aquatic system (Goodale et al., 2009; Ohte, 2012). On the contrary,  $\text{NH}_4^+$  is easily converted and emitted to the atmosphere via microbial activities in warm and humid conditions (Pajares and Bohannan, 2016; Lladó et al., 2017), which has lower retention in soil capacity compared to  $\text{NO}_3^-$ . Whether  $\text{NH}_4^+$  is source-limited casts a shadow of doubt on hydrologic control on  $\text{NH}_4^+$  transport.

#### 4.2.2. The Consideration of Landscape and Buffer Zone

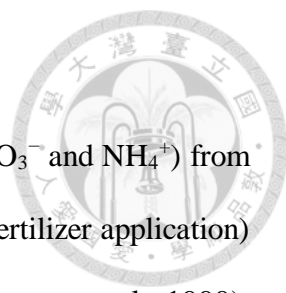
Streams receive nutrients from aquatic ecosystems and adjacent terrestrial landscapes, such that landscape configuration at watershed- or buffer zone-scale has important influences on stream water quality, ecological process and biodiversity. Watersheds with steeper slopes usually export more nutrients (Richards et al., 1996), yet our results surprisingly show that slope is negatively related to  $\text{NO}_3^-$  and  $\text{NH}_4^+$  exports (Figure 5). The possible reason is that most upstream watersheds with steep slopes are covered by pristine forests where anthropogenic sources are scarce (Johnson et al., 1997; Chang et al., 2018). Studies suggested that elevation might be a suitable parameter to predict water quality (Nava-López et al., 2016), but the collinearity between landscape (e.g., elevation or SLP) and human-made land cover (e.g., AGR and BD) from the high, steep montane region to the low, flat plain in Taiwan keeps us from using both simultaneously, even they might have significant contribution on nutrient exports.

Many studies demonstrate the control of land use and landscape on water quality at watershed scale (Varanka et al., 2012; Nava-López et al., 2016), but few studies consider



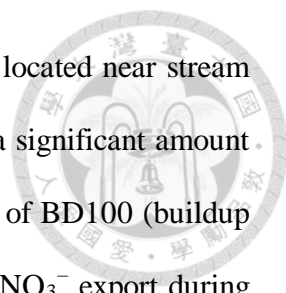
the distance from source area to river, i.e., the regulation of the riparian or buffer zone on nutrient movement. Plants and microbial activities within the riparian zone can help to uptake a great quantity of water, nutrients and sediments, mitigating the nutrients export to aquatic ecosystems within the watershed (Craig et al., 2008; Kaushal et al., 2008). However, the effective buffer distance is uncertain, and it could vary with the elements which are concerned (Gergel et al., 1999; Nielsen et al., 2012). A study conducted in Puerto Rico examined how the landscape pattern changes affected water quality in-stream and found that turbidity and dissolved oxygen responded to land use and land cover (LUC) at watershed scale (Uriarte et al., 2011), phosphorus concentration and fecal matter responded to LUC at sub-watershed scale, whereas nitrogen concentrations linked to LUC in riparian buffers of larger watersheds (Uriarte et al., 2011). Another study conducted in the Saginaw Bay of central Michigan investigating 62 catchments with a gradient of disturbed land cover showed that the land use factors within a 100 m buffer zone adjacent to the river could explain much higher (or equal) variance of  $\text{NO}_3^-$  and  $\text{NH}_4^+$  concentrations than those derived from the watershed scale (Johnson et al., 1997). Conversely, the relationships between total nitrogen exports and land use at the watershed scale were better than riparian buffer zones of 200 and 400 m in highly disturbed rivers in Illinois and Texas (Hunsaker and Levine, 1995). Previous assessments, based upon mountainous background, demonstrated that the buffer zone within a 100 m riparian zone, the buildup area particularly, plays an important role in regulating DIN exports (Hunsaker and Levine, 1995; Tong and Chen 2002; Meynendonckx et al., 2006). In Taiwan, the deficiency of sewage systems in buildup areas located near river networks contributes a significant amount to the DIN exports (Lee et al., 2014). The percentage of buildup at the watershed scale highlighted in our study indicates that dispersal non-point sewage sources in the buildup area and scattered agricultural activities would be critical in assessing  $\text{NH}_4^+$  export.

#### 4.2.3. Human Disturbance



The contribution of human activities to DIN exports (including  $\text{NO}_3^-$  and  $\text{NH}_4^+$ ) from land to water has been underscored due to agricultural activities (e.g., fertilizer application) and urbanization (e.g., domestic wastewater) (Johnson et al., 1997; Basnyat et al., 1999). To meet the ever-increasing demand, agricultural activities, such as high value fruit, montane cabbage and tea plantations, are pervasive in mountainous Taiwan. Consequently, the excessive addition of inorganic N fertilizer and organic manure on the thin soil layer is readily flushed out to aquatic ecosystems downstream during wet season (Chang et al., 1983; Huang et al., 2016). The N retention or removal capacity within watersheds will dramatically decrease if forests are transformed to agricultural areas (Shih et al., 2016). However, though the effects of agricultural land on  $\text{NO}_3^-$  and  $\text{NH}_4^+$  exports are statistically significant, their contributions are weaker than previous studies suggested (Tong and Chen 2002; Meynendonckx et. al., 2006). A Canadian study suggested that urban land use has a stronger effect on water quality than agriculture has (Sliva and Williams, 2001). Obviously, the importance of agricultural and urban land use on DIN exports is not easy to identify and separate, not only due to the area, but also the “intensity” (e.g., intensive agriculture or dense population) and spatial configuration. For example, the effect of urban areas is minor in Finland, because the population and settlements are mostly scattered so that wastewater can be purified before it flows into main streams (Varanka et al., 2012).

In this study, both  $\text{NO}_3^-$  and  $\text{NH}_4^+$  exports are significantly correlated to AGR and BD, which shows that AGR and BD are important for DIN exports (Figure 5). Notably, higher correlation coefficients of AGR and BD to  $\text{NH}_4^+$  export ( $r = 0.67 - 0.75$ ) than those to  $\text{NO}_3^-$  export ( $r = 0.32 - 0.40$ ) indicates that land use pattern is more effective to explain the variance of  $\text{NH}_4^+$  export. Conceptually,  $\text{NH}_4^+$  is easier to be taken up by plants and to be oxidized through nitrification and thus  $\text{NO}_3^-$  is the main species of DIN within

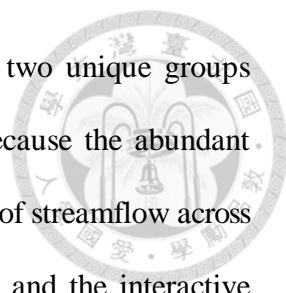


agriculture-dominated catchments. The intensive urban developments located near stream riparian in Taiwan deteriorates water quality directly and contributes a significant amount to the DIN exports. This phenomenon is reflected by the higher effect of BD100 (buildup area in a 100 m buffer zone) than the BD of the entire watershed on  $\text{NO}_3^-$  export during the dry season (Table 4). Therefore, domestic wastewater inevitably elevates  $\text{NH}_4^+$  export, which indicates a strong intrinsic collinearity with agriculture and buildup area. Such intrinsic collinearity presents an inseparable human-landscape system, and their interplay could not be distinguished perfectly.

#### 4.2.4. Interactive Effects among Variables

It was noticeable that interactive effects between landscape and human variables can explain most variabilities of  $\text{NO}_3^-$  export in the wet season (51.59% of the total variance) and seasonal  $\text{NH}_4^+$  export (both >80% of the total variance). Meanwhile, interactive effects between climatic and human variables explain 44.15% of the total  $\text{NO}_3^-$  export variance in the dry season. Thus, the interactive effect between landscape setting and human disturbance, and climatic and human disturbance will result in a high efficiency of prediction regarding  $\text{NO}_3^-$  and  $\text{NH}_4^+$  export in different conditions. One explanatory variable might be partially linked to other variables and altogether would improve or reduce the predictive power in evaluation of  $\text{NO}_3^-$  and  $\text{NH}_4^+$  export (Hough-Snee et al., 2015). For example, the opposite influences of streamflow and slope might suppress their capability to assess  $\text{NO}_3^-$  and  $\text{NH}_4^+$  exports without eliminating the collinearity between them. The mixed effects of environmental variables also suggest that it is necessary and will be more effective to apply an integrative management strategy (Aschonitis et al., 2016).

There is a significant change between the controlling interactive effects of  $\text{NO}_3^-$  export in the wet and dry seasons. In the wet season, streamflow and interactive effects between



landscape setting and human disturbance might reveal that they are two unique groups controlling the variance of  $\text{NO}_3^-$  export. This might be reasonable because the abundant rainfall during the humid summer will decrease the spatial variability of streamflow across Taiwan, which leads to a weaker relationship between streamflow and the interactive effects of landscape setting and human disturbance. On the contrary, the increase of the interactive effects between climatic and human disturbance might indicate the increasing spatial variability of streamflow in the dry season. Therefore, when we predict  $\text{NO}_3^-$  export in the wet season, both streamflow and the interactive effects between landscape setting and human disturbance cannot be ignored. Furthermore, the strong interactive effects between landscape setting and human disturbance on  $\text{NH}_4^+$  export, indicates that these two groups are the primary control of  $\text{NH}_4^+$  export. Because landscape setting and human disturbance are highly related (Figure 5), the variance explained by them might be similar and it might be difficult to separate their individual effect from both combined.

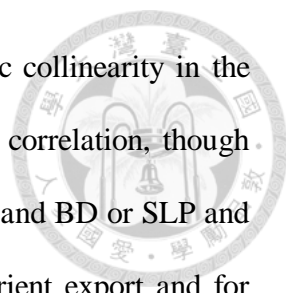
Some critical variables are not included in this study but might be significant in other regions. Studies found a strong negative relationship between nitrogen content and soil type (Sliva and Williams, 2001). However, most watersheds in Taiwan cross various soil substrates and geological units, which challenges us to unambiguously define a specific soil type for each watershed. In addition, long-lasting atmospheric nitrogen deposition could lead to N saturation in temperate forest ecosystems, resulting in net loss of nitrate to streams and consequent acidification of stream water (Aber et al., 1989, Aber et al., 1998, Howarth, 1998). A large-scale study indicated that riverine N export could be predicted by atmospheric N deposition rates (Howarth et al., 2002). Therefore, the influence of interaction between atmospheric deposition, land use and hydroclimate should be considered in following syntheses of DIN responses or developing models for riverine DIN export (Huang et al., 2014).



## 5. Conclusions



This work identified the major predictor variables and their interactive effects on DIN,  $\text{NO}_3^-$  and  $\text{NH}_4^+$  exports. Totally, 35 predictor variables among climatic, landscape setting and human disturbance dimensions were applied using PCA and pRDA analysis based upon data derived from 43 watersheds island-wide in Taiwan. Generally, the PCA identified that SF (Streamflow), SLP (average slope in watershed), AGR (percentage of the agriculture in the watershed), BD (percentage of the buildup area in watershed) and BD100 (percentage of buildup area in the 100 m buffer zone) are the main variables which can mostly explain the variances of DIN,  $\text{NO}_3^-$  and  $\text{NH}_4^+$  exports. Because nutrient export is the product of nutrient concentration and streamflow, streamflow, as expected, is the strongest predictor for  $\text{NO}_3^-$  export ( $r = 0.72$ ), but not for  $\text{NH}_4^+$  export, due to active biogeochemical processes. Meanwhile, the SLP ( $r = -0.75$ ) and BD ( $r = 0.75$ ) are equally best correlated to  $\text{NH}_4^+$  export. Based on the results of the pRDA model, five selected environmental variables can explain  $\text{NO}_3^-$  and  $\text{NH}_4^+$  export promisingly, but with different interactive effects. For  $\text{NO}_3^-$  export in the wet season, the climatic variable and human-landscape variables are independently responsive to most variances, while the dependent climatic-human variables present high marginal effects on  $\text{NO}_3^-$  exports in the dry season. The effective variables shift from human-landscape to climatic-human with seasons showing the mechanistic shift of nutrient transport. For  $\text{NH}_4^+$  export, the residual variances are 0.31 and 0.21 for the wet and dry seasons, respectively, and climatic variables (e.g., streamflow) are not effective variables for  $\text{NH}_4^+$  transport. The human-landscape variables are the major factors to explain the total variance of  $\text{NH}_4^+$  export (over 80%), in both the wet and dry seasons. The shift of interactive effects of variables on nutrient export is important for water quality management at watershed scale

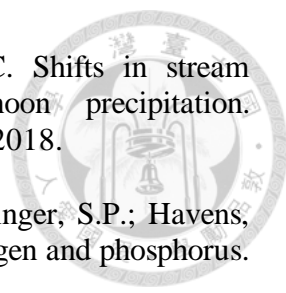


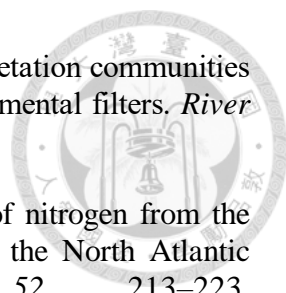
and designing mitigation strategies. Inevitably, the effects of intrinsic collinearity in the human-landscape system cannot be clearly separated due to spurious correlation, though the statistical approach provides some cues. For example, paired AGR and BD or SLP and BD are highly collinear but difficult to single out for estimating nutrient export and for interpretation. Nevertheless, with the accumulation of these studies, it is more possible to clarify the interactive effects, which could be of great help in advancing the understanding of DIN export mechanisms and global synthesized assessment.



## References

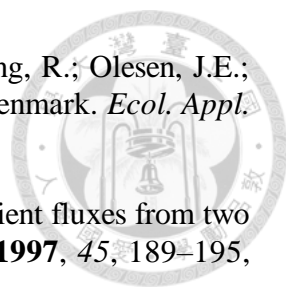
1. Aber, J.D.; Nadelhoffer, K.J.; Steudler, P.; Melillo, J.M. Nitrogen saturation in northern forest ecosystems. *Bioscience* **1989**, *39*, 378–286, doi:10.2307/1311067.
2. Aber, J.; McDowell, W.; Nadelhoffer, K.; Magill, A.; Berntson, G.; Kamakea, M.; McNulty, S.; Currie, W.; Rustad, L.; Fernandez, I. Nitrogen saturation in temperate forest ecosystems: Hypotheses revisited. *Bioscience* **1998**, *48*, 921–934, doi:10.2307/1313296.
3. Appling, A.P.; Leon, M.C.; McDowell, W.H. Reducing bias and quantifying uncertainty in watershed flux estimates: The R package loadflex. *Ecosphere* **2015**, *6*, 1–25, doi:10.1890/es14-00517.1.
4. Aschonitis, V.; Feld, C.; Castaldelli, G.; Turin, P.; Visonà, E.; Fano, E.A. Environmental stressor gradients hierarchically regulate macrozoobenthic community turnover in lotic systems of Northern Italy. *Hydrobiologia* **2016**, *765*, 131–147, doi:10.1007/s10750-015-2407-x.
5. Basnyat, P.; Teeter, L.D.; Flynn, K.M.; Lockaby, B.G. Relationships between landscape characteristics and nonpoint source pollution inputs to coastal estuaries. *Environ. Manag.* **1999**, *23*, 539–549, doi:10.1007/s002679900208.
6. Borcard, D.; Legendre, P.; Drapeau, P. Partialling out the spatial component of ecological variation. *Ecology* **1992**, *73*, 1045–1055, doi:10.2307/1940179.
7. Chang, M.; McCullough, J.D.; Granillo, A.B. Effects of land use and topography on some water quality variables in forested east Texas 1. *J. Am. Water Resour. Assoc.* **1983**, *19*, 191–196, doi:10.1111/j.1752-1688.1983.tb05313.x.
8. Chang, K.-H.; Jeng, F.-T.; Tsai, Y.-L.; Lin, P.-L. Modeling of long-range transport on Taiwan's acid deposition under different weather conditions. *Atmos. Environ.* **2000**, *34*, 3281–3295, doi:10.1016/s1352-2310(00)00072-8.
9. Chang, C.; Hamburg, S.; Hwong, J.; Lin, N.; Hsueh, M.; Chen, M.; Lin, T.-C. Impacts of tropical cyclones on hydrochemistry of a subtropical forest. *Hydrol. Earth Syst. Sci.* **2013**, *17*, 3815, doi:10.5194/hess-17-3815-2013.
10. Chang, C.-T.; Wang, S.-F.; Vadeboncoeur, M.A.; Lin, T.-C. Relating vegetation dynamics to temperature and precipitation at monthly and annual timescales in Taiwan using MODIS vegetation indices. *Int. J. Remote Sens.* **2014**, *35*, 598–620, doi:10.1080/01431161.2013.871593.
11. Chang, C.-T.; Wang, L.-J.; Huang, J.-C.; Liu, C.-P.; Wang, C.-P.; Lin, N.-H.; Wang, L.; Lin, T.-C. Precipitation controls on nutrient budgets in subtropical and tropical forests and the implications under changing climate. *Adv. Water Resour.* **2017**, *103*, 44–50, doi:10.1016/j.advwatres.2017.02.013.

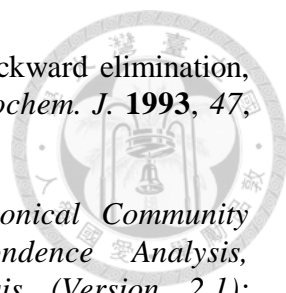
- 
12. Chang, C.T.; Huang, J.C.; Wang, L.; Shih, Y.T.; Lin, T.C. Shifts in stream hydrochemistry in responses to typhoon and non-typhoon precipitation. *Biogeosciences* **2018**, *15*, 2379–2391, doi:10.5194/bg-15-2379-2018.
  13. Conley, D.J.; Paerl, H.W.; Howarth, R.W.; Boesch, D.F.; Seitzinger, S.P.; Havens, K.E.; Lancelot, C.; Likens, G.E. Controlling eutrophication: Nitrogen and phosphorus. *Science* **2009**, *323*, 1014–1015, doi:10.1126/science.1167755.
  14. Craig, L.S.; Palmer, M.A.; Richardson, D.C.; Filoso, S.; Bernhardt, E.S.; Bledsoe, B.P.; Doyle, M.W.; Groffman, P.M.; Hassett, B.A.; Kaushal, S.S. Stream restoration strategies for reducing river nitrogen loads. *Front. Ecol. Environ.* **2008**, *6*, 529–538, doi:10.1890/070080.
  15. Ferguson, R. River loads underestimated by rating curves. *Water Resour. Res.* **1986**, *22*, 74–76, doi:10.1029/wr022i001p00074.
  16. Galloway, J.N.; Aber, J.D.; Erisman, J.W.; Seitzinger, S.P.; Howarth, R.W.; Cowling, E.B.; Cosby, B.J.; The Nitrogen Cascade. *BioScience*, **2003**, *53*, 341–356, doi:10.1641/0006-3568(2003)053[0341:TNC]2.0.CO;2.
  17. Galloway, J.N.; Dentener, F.J.; Capone, D.G.; Boyer, E.W.; Howarth, R.W.; Seitzinger, S.P.; Asner, G.P.; Cleveland, C.C.; Green, P.; Holland, E.A. Nitrogen cycles: Past, present, and future. *Biogeochemistry* **2004**, *70*, 153–226, doi:10.1007/s10533-004-0370-0.
  18. Gergel, S.E.; Turner, M.G.; Kratz, T.K. Dissolved organic carbon as an indicator of the scale of watershed influence on lakes and rivers. *Ecol. Appl.* **1999**, *9*, 1377–1390, doi:10.1890/1051-0761(1999)009[1377:DOCAAI]2.0.CO;2.
  19. Goodale, C.L.; Thomas, S.A.; Fredriksen, G.; Elliott, E.M.; Flinn, K.M.; Butler, T.J.; Walter, M.T. Unusual seasonal patterns and inferred processes of nitrogen retention in forested headwaters of the Upper Susquehanna River. *Biogeochemistry* **2009**, *93*, 197–218, doi:10.1007/s10533-009-9298-8.
  20. Graham, M.H. Confronting multicollinearity in ecological multiple regression. *Ecology* **2003**, *84*, 2809–2815, doi:10.1890/02-3114.
  21. Groffman, P.M.; Law, N.L.; Belt, K.T.; Band, L.E.; Fisher, G.T. Nitrogen fluxes and retention in urban watershed ecosystems. *Ecosystems* **2004**, *7*, 393–403, doi:10.1007/s10021-003-0039-x.
  22. Halbfuß, S.; Gebel, M.; Bürger, S. Modelling of long term nitrogen retention in surface waters. *Adv. Geosci.* **2010**, *27*, 145–148, doi:10.5194/adgeo-27-145-2010.
  23. He, B.; Kanae, S.; Oki, T.; Hirabayashi, Y.; Yamashiki, Y.; Takara, K. Assessment of global nitrogen pollution in rivers using an integrated biogeochemical modeling framework. *Water Res.* **2011**, *45*, 2573–2586, doi:10.1016/j.watres.2011.02.011.
  24. Hotelling, H. Analysis of a complex of statistical variables into principal components. *J. Educ. Psychol.* **1933**, *24*, 417, doi:10.1037/h0071325.

- 
25. Hough-Snee, N.; Roper, B.; Wheaton, J.; Lokteff, R. Riparian vegetation communities of the American Pacific Northwest are tied to multi-scale environmental filters. *River Res. Appl.* **2015**, *31*, 1151–1165, doi:10.1002/rra.2815.
  26. Howarth, R.W. An assessment of human influences on fluxes of nitrogen from the terrestrial landscape to the estuaries and continental shelves of the North Atlantic Ocean. *Nutr. Cycl. Agroecosyst.* **1998**, *52*, 213–223, doi:10.1023/A:1009784210657.
  27. Howarth, R.W.; Sharpley, A.; Walker, D. Sources of nutrient pollution to coastal waters in the United States: Implications for achieving coastal water quality goals. *Estuaries* **2002**, *25*, 656–676, doi:10.1007/bf02804898.
  28. Howarth, R.; Swaney, D.; Billen, G.; Garnier, J.; Hong, B.; Humborg, C.; Johnes, P.; Mörth, C.-M.; Marino, R. Nitrogen fluxes from the landscape are controlled by net anthropogenic nitrogen inputs and by climate. *Front. Ecol. Environ.* **2012**, *10*, 37–43, doi:10.1890/100178.
  29. Huang, H.; Chen, D.; Zhang, B.; Zeng, L.; Dahlgren, R.A. Modeling and forecasting riverine dissolved inorganic nitrogen export using anthropogenic nitrogen inputs, hydroclimate, and land-use change. *J. Hydrol.* **2014**, *517*, 95–104, doi:10.1016/j.jhydrol.2014.05.024.
  30. Huang, J.-C.; Kao, S.-J.; Lin, C.-Y.; Chang, P.-L.; Lee, T.-Y.; Li, M.-H. Effect of subsampling tropical cyclone rainfall on flood hydrograph response in a subtropical mountainous catchment. *J. Hydrol.* **2011**, *409*, 248–261, doi:10.1016/j.jhydrol.2011.08.037.
  31. Huang, J.-C.; Lee, T.-Y.; Kao, S.-J.; Hsu, S.-C.; Lin, H.-J.; Peng, T.-R. Land use effect and hydrological control on nitrate yield in subtropical mountainous watersheds. *Hydrol. Earth Syst. Sci.* **2012**, *16*, 699, doi:10.5194/hess-16-699-2012.
  32. Huang, J.-C.; Lee, T.-Y.; Lin, T.-C.; Hein, T.; Lee, L.-C.; Shih, Y.-T.; Kao, S.-J.; Shiah, F.-K.; Lin, N.-H. Effects of different N sources on riverine DIN export and retention in a subtropical high-standing island, Taiwan. *Biogeosciences* **2016**, *13*, 1787, doi:10.5194/bg-13-1787-2016.
  33. Hunsaker, C.T.; Levine, D.A. Hierarchical approaches to the study of water quality in rivers. *Bioscience* **1995**, *45*, 193–203, doi:10.2307/1312558.
  34. legendre, P.; legendre, L. Chapter 9—Ordination in reduced space. In *Developments in Environmental Modelling*; Legendre, P., Legendre, L., Eds.; Elsevier: Amsterdam, The Netherlands, 2012; Volume 24, pp. 425–520.
  35. Johnson, L.; Richards, C.; Host, G.; Arthur, J. Landscape influences on water chemistry in Midwestern stream ecosystems. *Freshw. Biol.* **1997**, *37*, 193–208, doi:10.1046/j.1365-2427.1997.d01-539.x.
  36. Johnson, R.K.; Furse, M.T.; Hering, D.; Sandin, L. Ecological relationships between stream communities and spatial scale: Implications for designing catchment-level

monitoring programmes. *Freshw. Biol.* **2007**, *52*, 939–958, doi:10.1111/j.1365-2427.2006.01692.x.

37. Jolliffe, I.T.; Cadima, J. Principal component analysis: A review and recent developments. *Philos. Trans. R. Soc. A* **2016**, *374*, 20150202, doi:10.1098/rsta.2015.0202.
38. Kaushal, S.S.; Groffman, P.M.; Mayer, P.M.; Striz, E.; Gold, A.J. Effects of stream restoration on denitrification in an urbanizing watershed. *Ecol. Appl.* **2008**, *18*, 789–804, doi:10.1890/07-1159.1.
39. Lee, T.-Y.; Huang, J.-C.; Kao, S.-J.; Tung, C.-P. Temporal variation of nitrate and phosphate transport in headwater catchments: The hydrological controls and land use alteration. *Biogeosciences* **2013**, *10*, 2617–2632, doi:10.5194/bg-10-2617-2013.
40. Lee, T.-Y.; Shih, Y.-T.; Huang, J.-C.; Kao, S.-J.; Shiah, F.-K.; Liu, K.-K. Speciation and dynamics of dissolved inorganic nitrogen export in the Danshui River, Taiwan. *Biogeosciences Discuss.* **2014**, *11*, 5307–5321, doi:10.5194/bg-11-5307-2014.
41. Legendre, P.; Oksanen, J.; ter Braak, C.J. Testing the significance of canonical axes in redundancy analysis. *Methods Ecol. Evol.* **2011**, *2*, 269–277, doi:10.1111/j.2041-210x.2010.00078.x.
42. Likens, G.E. *Biogeochemistry of a Forested Ecosystem*; Springer: Berlin/Heidelberg, Germany, 2013; doi:10.1007/978-1-4614-7810-2\_1.
43. Liu, Q. Variation partitioning by partial redundancy analysis (RDA). *Environmetrics* **1997**, *8*, 75–85, doi:10.1002/(sici)1099-095x(199703)8:23.0.co;2-n.
44. Lladó, S.; López-Mondéjar, R.; Baldrian, P. Forest Soil Bacteria: Diversity, Involvement in Ecosystem Processes, and Response to Global Change. *Microbiol. Mol. Biol. Rev.* **2017**, *81*, e00063–16, doi:10.1128/mmbr.00063-16.
45. McCrackin, M.L., Harrison, J.A., and Compton, J.E. Factors influencing export of dissolved inorganic nitrogen by major rivers: A new, seasonal, spatially explicit, global model. *Global Biogeochem. Cy.* **2014**, *28*, 269–285, doi:10.1002/2013GB004723.
46. Meynendonckx, J.; Heuvelmans, G.; Muys, B.; Feyen, J. Effects of watershed and riparian zone characteristics on nutrient concentrations in the River Scheldt Basin. *Hydrol. Earth Syst. Sci.* **2006**, *10*, 913–922, doi:10.5194/hess-10-913-2006.
47. Nash, J.E.; Sutcliffe, J.V. River flow forecasting through conceptual models part I—A discussion of principles. *J. Hydrol.* **1970**, *10*, 282–290, doi:10.1016/0022-1694(70)90255-6.
48. Nava-López, M.Z.; Diemont, S.A.; Hall, M.; Ávila-Akerberg, V. Riparian buffer zone and whole watershed influences on river water Quality: Implications for ecosystem services near megacities. *Environ. Process.* **2016**, *3*, 277–305, doi:10.1007/s40710-016-0145-3.

- 
49. Nielsen, A.; Trolle, D.; Søndergaard, M.; Lauridsen, T.L.; Bjerring, R.; Olesen, J.E.; Jeppesen, E. Watershed land use effects on lake water quality in Denmark. *Ecol. Appl.* **2012**, *22*, 1187–1200, doi:10.1890/11-1831.1.
50. Ohowa, B.; Mwashote, B.; Shimbira, W. Dissolved inorganic nutrient fluxes from two seasonal rivers into Gazi Bay, Kenya. *Estuar. Coast. Shelf Sci.* **1997**, *45*, 189–195, doi:10.1006/ecss.1996.0187.
51. Ohte, N. Implications of seasonal variation in nitrate export from forested ecosystems: A review from the hydrological perspective of ecosystem dynamics. *Ecol. Res.* **2012**, *27*, 657–665, doi:10.1007/s11284-012-0956-2.
52. Pajares, S.; Bohannan, B.J. Ecology of nitrogen fixing, nitrifying, and denitrifying microorganisms in tropical forest soils. *Front. Microbiol.* **2016**, *7*, 1045, doi:10.3389/fmicb.2016.01045.
53. Parajka, J.; Viglione, A.; Rogger, M.; Salinas, J.L.; Sivapalan, M.; Blöschl, G. Comparative assessment of predictions in ungauged basins &ndash; Part 1: Runoff-hydrograph studies. *Hydrol. Earth Syst. Sci.* **2013**, *17*, 1783–1795, doi:10.5194/hess-17-1783-2013.
54. Porterfield, G. *Computation of Fluvial-Sediment Discharge*; US Government Printing Office: Washington, DC, USA, 1972; doi:10.3133/twri03C3.
55. Richards, C.; Johnson, L.B.; Host, G.E. Landscape-scale influences on stream habitats and biota. *Can. J. Fish. Aquat. Sci.* **1996**, *53*, 295–311, doi:10.1139/f96-006.
56. Robertson, D.M.; Roerish, E.D. Influence of various water quality sampling strategies on load estimates for small streams. *Water Resour. Res.* **1999**, *35*, 3747–3759, doi:10.1029/1999wr900277.
57. Rockström, J.; Steffen, W.; Noone, K.; Persson, Å.; Chapin, F.S.; Lambin, E.F.; Lenton, T.M.; Scheffer, M.; Folke, C.; Schellnhuber, H.J. A safe operating space for humanity. *Nature* **2009**, *461*, 472–475, doi:10.1038/461472a.
58. Seitzinger, S.P.; Mayorga, E.; Bouwman, A.F.; Kroeze, C.; Beusen, A.H.W.; Billen, G.; Van Drecht, G.; Dumont, E.; Fekete, B.M.; Garnier, J., et al. Global river nutrient export: A scenario analysis of past and future trends. *Glob. Biogeochem. Cycle* **2010**, *24*, GB0A08, doi:doi:10.1029/2009GB003587.
59. Shih, Y.-T.; Lee, T.-Y.; Huang, J.-C.; Kao, S.-J. Apportioning riverine DIN load to export coefficients of land uses in an urbanized watershed. *Sci. Total Environ.* **2016**, *560*, 1–11, doi:10.1016/j.scitotenv.2016.04.055.
60. Sliva, L.; Williams, D.D. Buffer zone versus whole catchment approaches to studying land use impact on river water quality. *Water Res.* **2001**, *35*, 3462–3472, doi:10.1016/s0043-1354(01)00062-8.

- 
61. Sutter, J.M.; Kalivas, J.H. Comparison of forward selection, backward elimination, and generalized simulated annealing for variable selection. *Microchem. J.* **1993**, *47*, 60–66, doi:10.1006/mchj.1993.1012.
62. ter Braak, C.J. *CANOCO-a FORTRAN Program. for Canonical Community Ordination By [Partial][Etrended][Canonical] Correspondence Analysis, Principal Components Analysis and Redundancy Analysis (Version 2.1)*; Wageningen University: Wageningen, The Netherlands, 1988.
63. Tong, S.T.; Chen, W. Modeling the relationship between land use and surface water quality. *J. Environ. Manag.* **2002**, *66*, 377–393, doi:10.1006/jema.2002.0593.
64. Tørseth, K.; Aas, W.; Breivik, K.; Fjæ raa, A.M.; Fiebig, M.; Hjellbrekke, A.-G.; Lund Myhre, C.; Solberg, S.; Yttri, K.E. Introduction to the European Monitoring and Evaluation Programme (EMEP) and observed atmospheric composition change during 1972–2009. *Atmos. Chem. Phys.* **2012**, *12*, 5447–5481, doi:10.5194/acp-12-5447-2012.
65. Uriarte, M.; Yackulic, C.B.; Lim, Y.; Arce-Nazario, J.A. Influence of land use on water quality in a tropical landscape: A multi-scale analysis. *Landsc. Ecol.* **2011**, *26*, 1151, doi:10.1007/s10980-011-9642-y.
66. Varanka, S.; Luoto, M. Environmental determinants of water quality in boreal rivers based on partitioning methods. *River Res. Appl.* **2012**, *28*, 1034–1046, doi:10.1002/rra.1502.
67. Vet, R.; Artz, R.S.; Carou, S.; Shaw, M.; Ro, C.-U.; Aas, W.; Baker, A.; Bowersox, V.C.; Dentener, F.; Galy-Lacaux, C. A global assessment of precipitation chemistry and deposition of sulfur, nitrogen, sea salt, base cations, organic acids, acidity and pH, and phosphorus. *Atmos. Environ.* **2014**, *93*, 3–100, doi:10.1016/j.atmosenv.2013.10.060.
68. Xiao, R.; Wang, G.; Zhang, Q.; Zhang, Z. Multi-scale analysis of relationship between landscape pattern and urban river water quality in different seasons. *Sci. Rep.* **2016**, *6*, 1–10, doi:10.1038/srep25250.



## SUPPLEMENTARY MATERIALS



**Table S1.** The basic landscape characteristics of the 43 sampling sites.

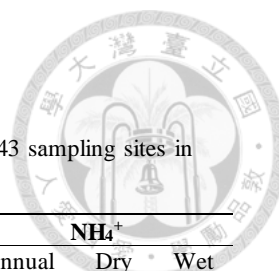
Station Name	Watershed characteristic					Land use		
	Area (km <sup>2</sup> )	Average Temperature (°C)	Average Slope (%)	Average Flow (mm)	Average Rainfall (mm)	Forest (%)	Agri. (%)	Buildup (%)
1. Wu-Tu	198	20.9	35	4258	4857	83	3	8
2. Po-Bridge	111	21.6	39	3876	3988	76	8	11
3. San-Hsia	126	20.8	44	2122	2733	80	13	4
4. Hsin-Pu	210	21.2	26	1411	2031	60	21	9
5. Nei-Wan	147	20.0	54	2961	3001	90	4	2
6. Shang-Ping	212	17.1	61	2200	2770	93	3	1
7. Ping-An-Bridge	297	20.1	42	1485	2254	80	10	4
8. Yun-Hsin-Chou	146	19.0	54	2264	2767	92	3	1
9. Pei-Shih Bridge	475	19.7	41	842	1591	74	14	5
10. I-Li	629	16.5	64	976	1759	83	6	1
11. Lung-An Bridge	969	15.5	69	848	2347	86	6	1
12. Chi-Nan Bridge	266	21.4	26	1616	1840	42	29	18
13. Yu-Feng Bridge	2096	18.3	67	1682	2443	85	4	1
14. Chi-Chou Bridge	2969	18.7	59	1093	2023	76	10	2
15. Pei-Kang-2	220	22.1	9	1704	2275	18	53	18
16. Tun-Kun Bridge	578	22.0	8	1068	1765	12	65	15
17. Chun-Huei Bridge	115	19.2	42	2061	3131	58	26	5
18. Chu-Kuo	81	18.5	53	2800	3607	70	21	2
19. Ho-Sung Bridge	440	21.2	20	3111	3768	23	57	10
20. Shin-Ying	225	22.3	19	1786	2840	36	47	7
21. Yu-Tien	159	22.1	37	1077	2413	68	21	2
22. Hsin-Shih	142	23.4	11	1500	2612	33	42	14
23. A-Lien-2	176	23.6	21	1724	2943	59	21	5
24. Chung-Te	140	23.6	21	1903	3024	57	22	5
25. Li-Lin Bridge	2869	20.3	54	1879	3546	77	12	2
26. Liu-Kwei	890	18.1	65	2600	3870	85	4	1
28. San-Ti-Men	409	21.8	65	3542	4737	93	2	1
31. Chih-Pen	164	23.4	58	2223	3592	93	3	1
32. Li-Chia	147	20.2	63	2121	3856	95	1	0
33. Tai-Tung Bridge	1574	17.5	56	1685	3680	59	19	1
34. Yen-Ping	469	18.0	64	1740	3388	69	10	0
35. Hsin-Wu-Lu	628	16.1	64	2021	3208	60	17	0
36. Yu-Li Bridge	999	19.9	57	1754	2889	81	8	1
37. Jui-Sui Bridge	1528	20.4	55	2463	3367	80	9	1
38. His-Po Bridge	240	20.7	69	2495	4084	88	1	0
39. Ping-Lin	210	20.1	76	1330	3015	87	1	0
40. Jen-Shou Bridge	441	17.0	71	2181	3358	90	1	0
41. Hua-Lien Bridge	1497	19.8	57	2876	4044	76	11	2
42. Lu-Shui	433	14.9	74	3129	3667	90	1	0
43. Chi-Neng-Pu	536	17.6	67	2983	3524	91	0	0
44. Jhong-Yue	136	21.2	60	3156	3052	95	2	0
45. Niu-Tou	453	15.0	60	1788	3059	89	2	0
46. Lan-Yang Bridge	823	17.3	50	2361	3111	79	9	2

The Agri. indicates agriculture.



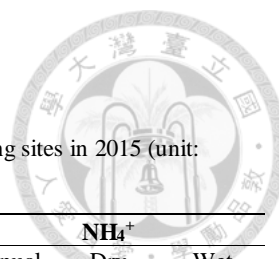
**Table S2.** Estimated annual and seasonal DIN, NO<sub>3</sub><sup>-</sup> and NH<sub>4</sub><sup>+</sup> concentrations for 43 sampling sites in 2015 (unit: mg-N L<sup>-1</sup>).

2015 Station Name	DIN			NO <sub>3</sub> <sup>-</sup>			NH <sub>4</sub> <sup>+</sup>		
	Annual	Dry	Wet	Annual	Dry	Wet	Annual	Dry	Wet
1. Wu-Tu	2.51	2.77	2.31	1.36	1.55	1.20	1.04	1.07	1.02
2. Po-Bridge	2.25	2.87	2.10	1.19	1.26	1.18	0.96	1.43	0.84
3. San-Hsia	2.27	1.96	2.31	1.45	0.59	1.59	0.76	1.24	0.69
4. Hsin-Pu	2.09	2.54	1.98	1.55	1.93	1.45	0.46	0.49	0.45
5. Nei-Wan	0.91	0.67	0.94	0.77	0.63	0.80	0.13	0.04	0.15
6. Shang-Ping	0.66	0.44	0.73	0.64	0.39	0.71	0.03	0.05	0.02
7. Ping-An-Bridge	1.08	0.75	1.10	0.89	0.61	0.91	0.14	0.08	0.14
8. Yun-Hsin-Chou	0.80	0.62	0.84	0.79	0.61	0.83	0.01	0.01	0.01
9. Pei-Shih Bridge	2.12	2.99	2.06	1.51	1.42	1.52	0.50	1.33	0.44
10. I-Li	1.57	1.73	1.56	1.47	1.45	1.48	0.05	0.27	0.03
11. Lung-An Bridge	1.38	0.97	1.48	1.18	0.62	1.31	0.19	0.34	0.16
12. Chi-Nan Bridge	4.15	4.94	3.74	2.20	2.07	2.27	1.65	2.51	1.20
13. Yu-Feng Bridge	0.96	0.80	1.03	0.60	0.41	0.67	0.34	0.35	0.33
14. Chi-Chou Bridge	2.06	1.47	2.11	1.28	0.44	1.35	0.74	0.96	0.72
15. Pei-Kang-2	5.68	6.61	5.40	1.64	1.26	1.75	3.78	5.13	3.37
16. Tun-Kun Bridge	8.87	7.58	9.51	2.66	1.22	3.39	4.59	6.14	3.81
17. Chun-Huei Bridge	2.01	2.47	1.96	1.40	1.07	1.43	0.57	1.29	0.49
18. Chu-Kuo	2.25	4.81	2.06	1.60	0.31	1.70	0.65	4.50	0.36
19. Ho-Sung Bridge	3.07	5.27	2.91	1.62	1.27	1.64	1.18	3.46	1.01
20. Shin-Ying	3.85	4.94	3.63	2.20	1.69	2.30	1.42	2.95	1.11
21. Yu-Tien	2.00	1.36	2.03	1.92	1.29	1.95	0.03	0.02	0.03
22. Hsin-Shih	4.99	9.74	4.37	1.17	0.46	1.26	3.35	9.13	2.59
23. A-Lien-2	3.95	6.70	3.67	1.15	0.90	1.18	2.52	5.37	2.23
24. Chung-Te	4.73	6.74	4.56	1.38	1.17	1.40	2.99	4.98	2.82
25. Li-Lin Bridge	0.76	0.83	0.75	0.67	0.66	0.68	0.05	0.09	0.04
26. Liu-Kwei	0.43	0.24	0.47	0.40	0.22	0.45	0.02	0.02	0.02
28. San-Ti-Men	0.81	0.16	0.82	0.77	0.14	0.79	0.03	0.01	0.04
31. Chih-Pen	0.55	0.45	0.60	0.41	0.29	0.46	0.11	0.11	0.11
32. Li-Chia	0.57	0.37	0.63	0.55	0.35	0.61	0.01	0.01	0.01
33. Tai-Tung Bridge	0.73	0.61	0.78	0.65	0.52	0.70	0.05	0.05	0.05
34. Yen-Ping	0.50	0.42	0.53	0.37	0.28	0.42	0.10	0.11	0.09
35. Hsin-Wu-Lu	0.39	0.35	0.41	0.32	0.29	0.33	0.04	0.04	0.05
36. Yu-Li Bridge	0.53	0.48	0.56	0.46	0.43	0.48	0.06	0.05	0.08
37. Jui-Sui Bridge	0.53	0.54	0.52	0.45	0.44	0.45	0.04	0.06	0.03
38. His-Po Bridge	0.58	0.59	0.58	0.46	0.45	0.46	0.09	0.11	0.07
39. Ping-Lin	0.35	0.32	0.36	0.33	0.30	0.34	0.02	0.02	0.02
40. Jen-Shou Bridge	0.42	0.36	0.43	0.39	0.33	0.41	0.02	0.03	0.02
41. Hua-Lien Bridge	0.81	0.81	0.81	0.73	0.72	0.73	0.04	0.05	0.04
42. Lu-Shui	0.47	0.36	0.52	0.45	0.34	0.50	0.02	0.02	0.02
43. Chi-Neng-Pu	0.84	0.73	0.88	0.30	0.27	0.30	0.54	0.44	0.57
44. Jhong-Yue	0.46	0.36	0.48	0.43	0.35	0.46	0.02	0.01	0.02
45. Niu-Tou	0.58	0.46	0.62	0.56	0.44	0.59	0.02	0.01	0.02
46. Lan-Yang Bridge	1.09	1.25	1.01	0.61	0.62	0.60	0.45	0.58	0.39



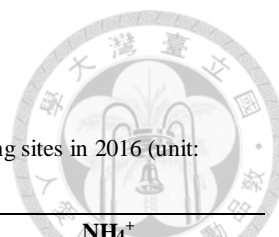
**Table S3.** Estimated annual and seasonal DIN, NO<sub>3</sub><sup>-</sup> and NH<sub>4</sub><sup>+</sup> concentrations for 43 sampling sites in 2016 (unit: mg-N L<sup>-1</sup>).

2016 Station Name	DIN			NO <sub>3</sub> <sup>-</sup>			NH <sub>4</sub> <sup>+</sup>		
	Annual	Dry	Wet	Annual	Dry	Wet	Annual	Dry	Wet
1. Wu-Tu	1.93	2.05	1.83	1.20	1.37	1.06	0.66	0.59	0.71
2. Po-Bridge	1.79	1.95	1.69	1.21	1.29	1.17	0.50	0.57	0.45
3. San-Hsia	1.84	1.70	1.91	1.32	1.17	1.39	0.46	0.48	0.44
4. Hsin-Pu	1.55	1.68	1.47	1.31	1.42	1.24	0.19	0.21	0.18
5. Nei-Wan	0.76	0.72	0.78	0.74	0.70	0.76	0.02	0.02	0.02
6. Shang-Ping	0.83	0.70	0.99	0.79	0.68	0.93	0.04	0.02	0.06
7. Ping-An-Bridge	1.05	1.03	1.06	0.93	0.91	0.96	0.08	0.09	0.07
8. Yun-Hsin-Chou	0.80	0.79	0.82	0.79	0.78	0.81	0.01	0.01	0.01
9. Pei-Shih Bridge	1.71	1.65	1.78	1.39	1.39	1.39	0.22	0.18	0.28
10. I-Li	1.26	1.23	1.28	1.21	1.20	1.24	0.03	0.03	0.03
11. Lung-An Bridge	1.56	0.88	1.75	1.37	0.82	1.53	0.18	0.05	0.21
12. Chi-Nan Bridge	3.55	3.88	3.31	2.15	2.15	2.15	1.15	1.46	0.92
13. Yu-Feng Bridge	0.81	0.75	0.84	0.65	0.60	0.69	0.14	0.14	0.14
14. Chi-Chou Bridge	1.45	1.12	1.55	1.24	0.86	1.36	0.18	0.23	0.16
15. Pei-Kang-2	4.61	4.75	4.55	1.80	1.47	1.94	2.56	3.05	2.34
16. Tun-Kun Bridge	8.91	6.39	10.45	2.79	1.50	3.58	3.49	4.66	2.78
17. Chun-Huei Bridge	1.77	2.05	1.72	1.40	1.31	1.42	0.34	0.68	0.28
18. Chu-Kuo	1.90	1.17	2.03	1.69	0.63	1.89	0.20	0.54	0.14
19. Ho-Sung Bridge	2.85	3.92	2.60	1.67	1.51	1.70	0.95	2.07	0.68
20. Shin-Ying	3.03	4.28	2.71	2.08	2.19	2.05	0.75	1.82	0.49
21. Yu-Tien	1.36	1.27	1.37	1.31	1.23	1.31	0.04	0.02	0.04
22. Hsin-Shih	4.24	5.62	3.94	1.38	1.03	1.46	2.21	4.30	1.75
23. A-Lien-2	2.89	3.87	2.71	1.18	1.11	1.19	1.45	2.51	1.26
24. Chung-Te	2.94	3.87	2.79	1.36	1.18	1.39	1.32	2.40	1.15
25. Li-Lin Bridge	0.73	0.60	0.76	0.67	0.52	0.69	0.05	0.06	0.05
26. Liu-Kwei	0.37	0.29	0.42	0.34	0.25	0.38	0.03	0.03	0.03
28. San-Ti-Men	0.83	0.40	0.87	0.77	0.36	0.81	0.05	0.03	0.05
31. Chih-Pen	0.58	0.38	0.63	0.51	0.29	0.56	0.06	0.07	0.06
32. Li-Chia	0.54	0.36	0.57	0.52	0.34	0.55	0.02	0.01	0.02
33. Tai-Tung Bridge	0.69	0.61	0.71	0.57	0.53	0.58	0.10	0.05	0.11
34. Yen-Ping	0.44	0.35	0.46	0.35	0.25	0.38	0.08	0.08	0.08
35. Hsin-Wu-Lu	0.35	0.31	0.37	0.26	0.25	0.26	0.09	0.05	0.10
36. Yu-Li Bridge	0.51	0.45	0.52	0.46	0.41	0.47	0.05	0.04	0.05
37. Jui-Sui Bridge	0.47	0.49	0.47	0.43	0.42	0.43	0.03	0.04	0.03
38. His-Po Bridge	0.39	0.45	0.36	0.30	0.35	0.27	0.07	0.08	0.07
39. Ping-Lin	0.28	0.28	0.28	0.26	0.26	0.25	0.02	0.02	0.02
40. Jen-Shou Bridge	0.31	0.31	0.31	0.29	0.29	0.29	0.01	0.01	0.01
41. Hua-Lien Bridge	0.74	0.74	0.74	0.67	0.68	0.67	0.05	0.04	0.06
42. Lu-Shui	0.45	0.38	0.48	0.42	0.36	0.45	0.02	0.02	0.02
43. Chi-Neng-Pu	0.44	0.33	0.47	0.26	0.22	0.27	0.17	0.11	0.19
44. Jhong-Yue	0.46	0.30	0.50	0.44	0.28	0.48	0.02	0.01	0.02
45. Niu-Tou	0.56	0.49	0.61	0.54	0.47	0.59	0.01	0.01	0.01
46. Lan-Yang Bridge	0.71	0.68	0.73	0.60	0.57	0.61	0.09	0.08	0.10



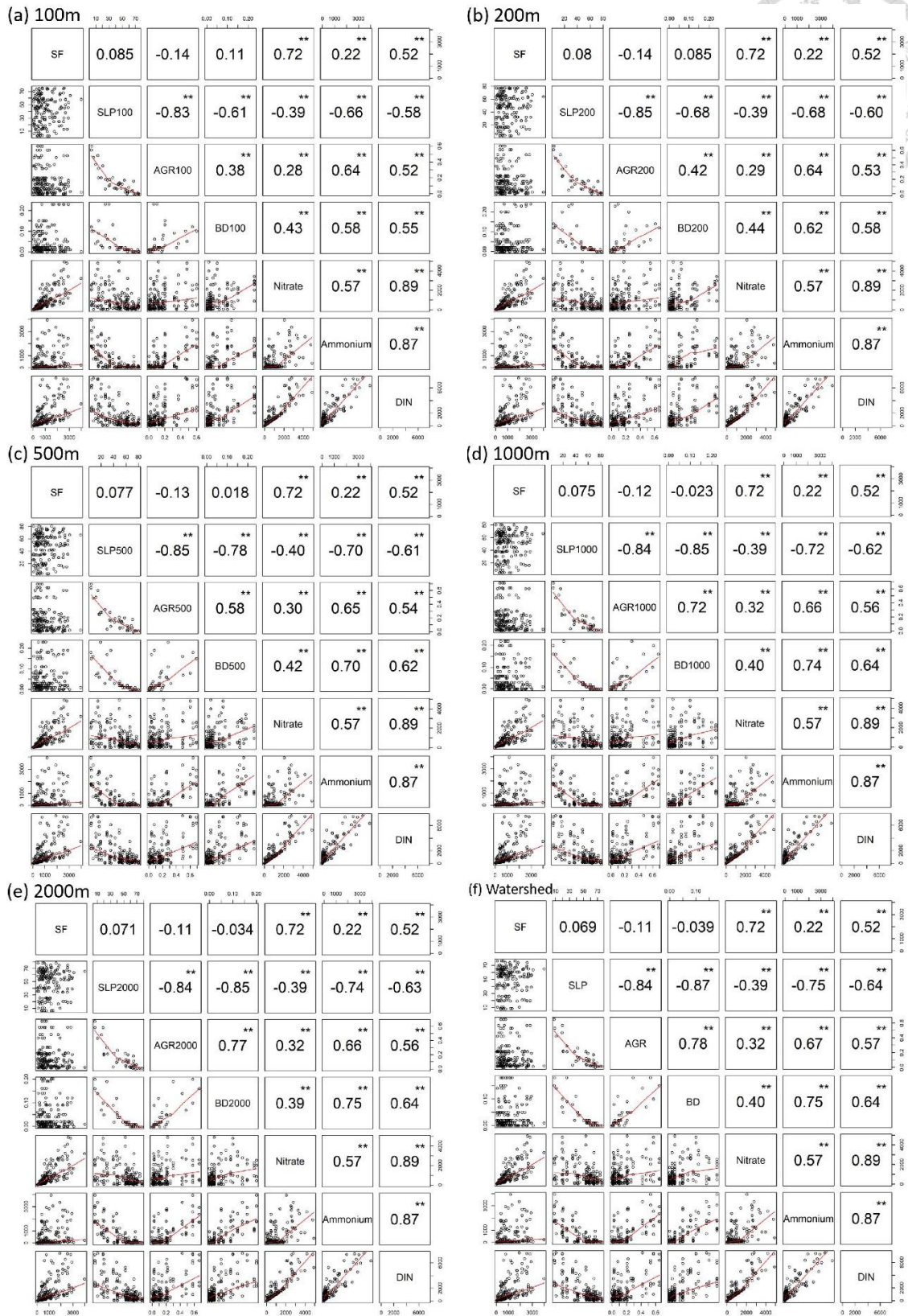
**Table S4.** Estimated annual and seasonal DIN, NO<sub>3</sub><sup>-</sup> and NH<sub>4</sub><sup>+</sup> exports for 43 sampling sites in 2015 (unit: kg-N km<sup>-2</sup> yr<sup>-1</sup>).

2015 Station Name	DIN			NO <sub>3</sub> <sup>-</sup>			NH <sub>4</sub> <sup>+</sup>		
	Annual	Dry	Wet	Annual	Dry	Wet	Annual	Dry	Wet
1. Wu-Tu	9716.71	4730.03	4986.69	5251.62	2657.45	2594.17	4032.04	1823.26	2208.78
2. Po-Bridge	8149.36	2051.85	6097.51	4324.16	897.03	3427.13	3457.11	1024.81	2432.30
3. San-Hsia	4596.03	532.95	4063.08	2945.93	160.76	2785.17	1543.94	335.89	1208.05
4. Hsin-Pu	2148.27	533.99	1614.28	1587.06	405.15	1181.91	471.97	103.04	368.92
5. Nei-Wan	2777.96	264.68	2513.28	2364.10	248.57	2115.53	404.55	14.90	389.65
6. Shang-Ping	1135.58	174.50	961.08	1085.60	155.19	930.41	44.13	18.01	26.12
7. Ping-An-Bridge	1140.62	41.08	1099.55	942.43	33.36	909.07	149.36	4.48	144.88
8. Yun-Hsin-Chou	1401.07	171.11	1229.96	1381.66	167.76	1213.89	14.10	2.50	11.60
9. Pei-Shih Bridge	1289.23	114.12	1175.10	921.65	54.06	867.60	302.71	50.53	252.18
10. I-Li	1500.99	115.70	1385.29	1406.19	96.47	1309.71	49.19	18.13	31.06
11. Lung-An Bridge	857.85	118.90	738.95	730.99	76.38	654.61	120.63	42.06	78.57
12. Chi-Nan Bridge	5703.13	2319.58	3383.55	3031.06	973.38	2057.68	2262.53	1179.46	1083.07
13. Yu-Feng Bridge	956.11	234.62	721.49	591.48	120.87	470.61	332.82	103.17	229.64
14. Chi-Chou Bridge	1467.35	78.32	1389.03	909.48	23.23	886.25	526.75	50.96	475.79
15. Pei-Kang-2	8655.88	2336.25	6319.63	2495.31	446.42	2048.90	5757.24	1815.02	3942.21
16. Tun-Kun Bridge	10228.53	2928.19	7300.34	3069.35	471.44	2597.91	5295.93	2372.08	2923.85
17. Chun-Huei Bridge	3993.16	460.76	3532.39	2776.41	199.98	2576.43	1125.29	239.93	885.36
18. Chu-Kuo	5676.69	855.25	4821.44	4037.10	55.22	3981.88	1630.81	798.61	832.20
19. Ho-Sung Bridge	8423.14	1014.76	7408.38	4430.78	244.68	4186.10	3227.25	665.71	2561.54
20. Shin-Ying	5348.58	1156.47	4192.11	3052.76	395.20	2657.56	1968.95	689.68	1279.27
21. Yu-Tien	1351.23	38.85	1312.38	1297.32	36.90	1260.42	22.29	0.57	21.73
22. Hsin-Shih	3372.15	760.94	2611.21	786.61	35.71	750.90	2259.05	713.22	1545.83
23. A-Lien-2	3510.56	555.23	2955.33	1021.13	74.89	946.23	2238.02	445.08	1792.95
24. Chung-Te	5129.99	559.25	4570.74	1496.72	97.24	1399.47	3241.01	413.65	2827.36
25. Li-Lin Bridge	892.00	122.51	769.49	792.07	97.99	694.07	59.11	13.92	45.19
26. Liu-Kwei	777.39	87.37	690.02	731.07	79.76	651.32	38.67	6.44	32.23
28. San-Ti-Men	2213.22	7.82	2205.40	2108.81	7.13	2101.68	94.51	0.53	93.99
31. Chih-Pen	645.26	158.55	486.71	474.42	102.00	372.42	127.11	37.65	89.46
32. Li-Chia	402.18	60.09	342.09	390.84	57.42	333.42	9.18	2.17	7.01
33. Tai-Tung Bridge	1067.90	270.92	796.98	947.42	231.04	716.38	74.43	21.91	52.52
34. Yen-Ping	463.58	123.99	339.59	347.72	81.08	266.64	89.85	33.10	56.75
35. Hsin-Wu-Lu	416.62	124.10	292.52	342.13	101.70	240.42	47.35	13.42	33.93
36. Yu-Li Bridge	318.93	133.68	185.25	276.05	118.42	157.63	39.32	13.52	25.81
37. Jui-Sui Bridge	778.94	239.78	539.15	658.66	194.73	463.93	58.52	25.09	33.43
38. His-Po Bridge	734.86	288.43	446.43	576.62	218.81	357.80	107.64	51.71	55.93
39. Ping-Lin	227.01	23.04	203.97	212.23	21.52	190.71	12.83	1.30	11.53
40. Jen-Shou Bridge	621.19	98.82	522.37	587.67	90.97	496.70	28.98	7.02	21.96
41. Hua-Lien Bridge	1535.52	554.04	981.48	1383.95	494.27	889.67	79.59	32.14	47.45
42. Lu-Shui	1219.21	271.85	947.36	1159.83	254.23	905.61	51.56	15.32	36.24
43. Chi-Neng-Pu	1813.06	366.13	1446.93	637.16	137.60	499.56	1155.22	223.62	931.59
44. Jhong-Yue	1039.55	195.86	843.69	989.74	186.49	803.24	42.86	7.73	35.14
45. Niu-Tou	796.83	134.19	662.64	767.89	128.95	638.94	21.80	4.21	17.60
46. Lan-Yang Bridge	2610.60	958.63	1651.97	1459.61	477.56	982.05	1085.13	446.47	638.67

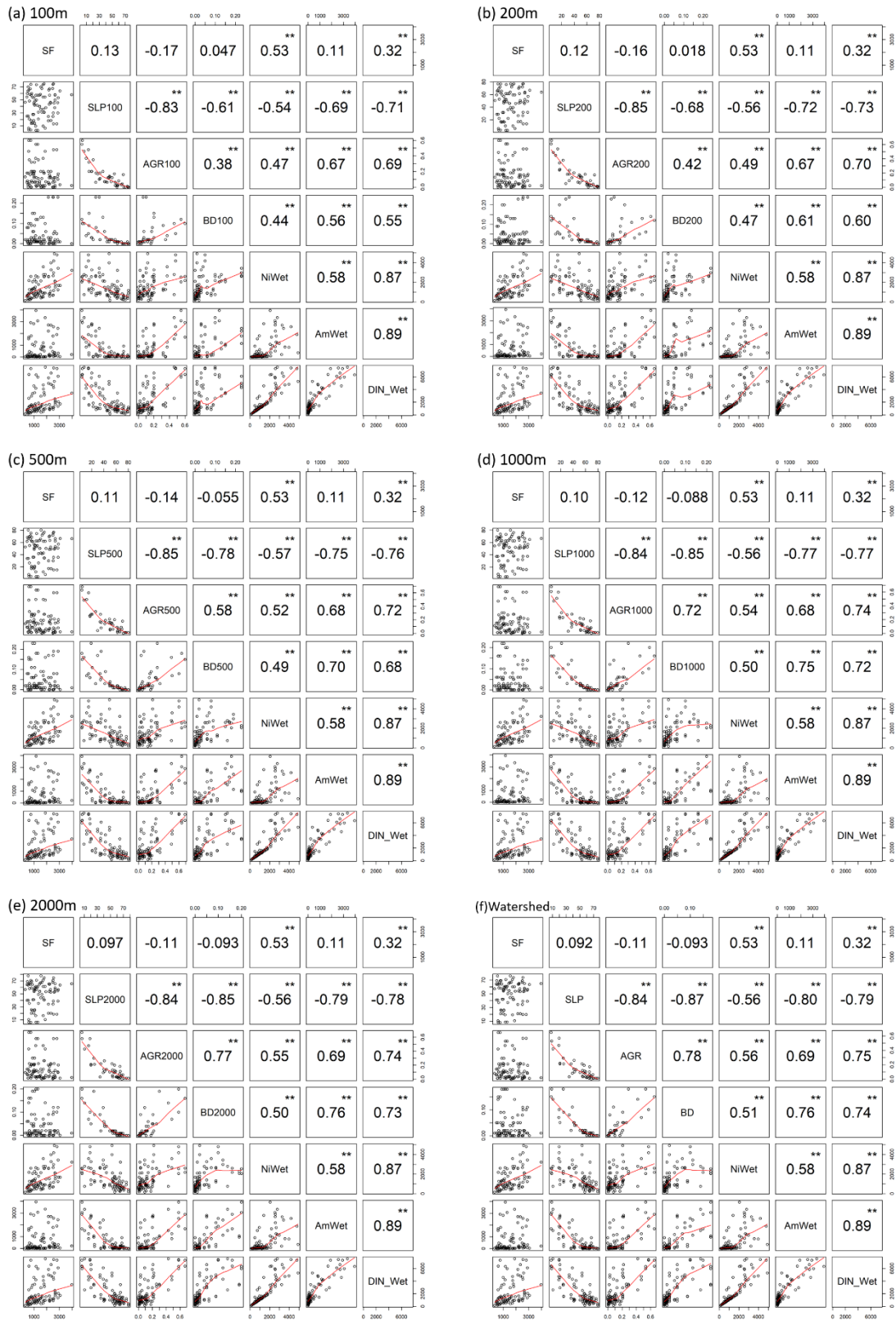


**Table S5.** Estimated annual and seasonal DIN, NO<sub>3</sub><sup>-</sup> and NH<sub>4</sub><sup>+</sup> exports for 43 sampling sites in 2016 (unit: kg-N km<sup>-2</sup> yr<sup>-1</sup>).

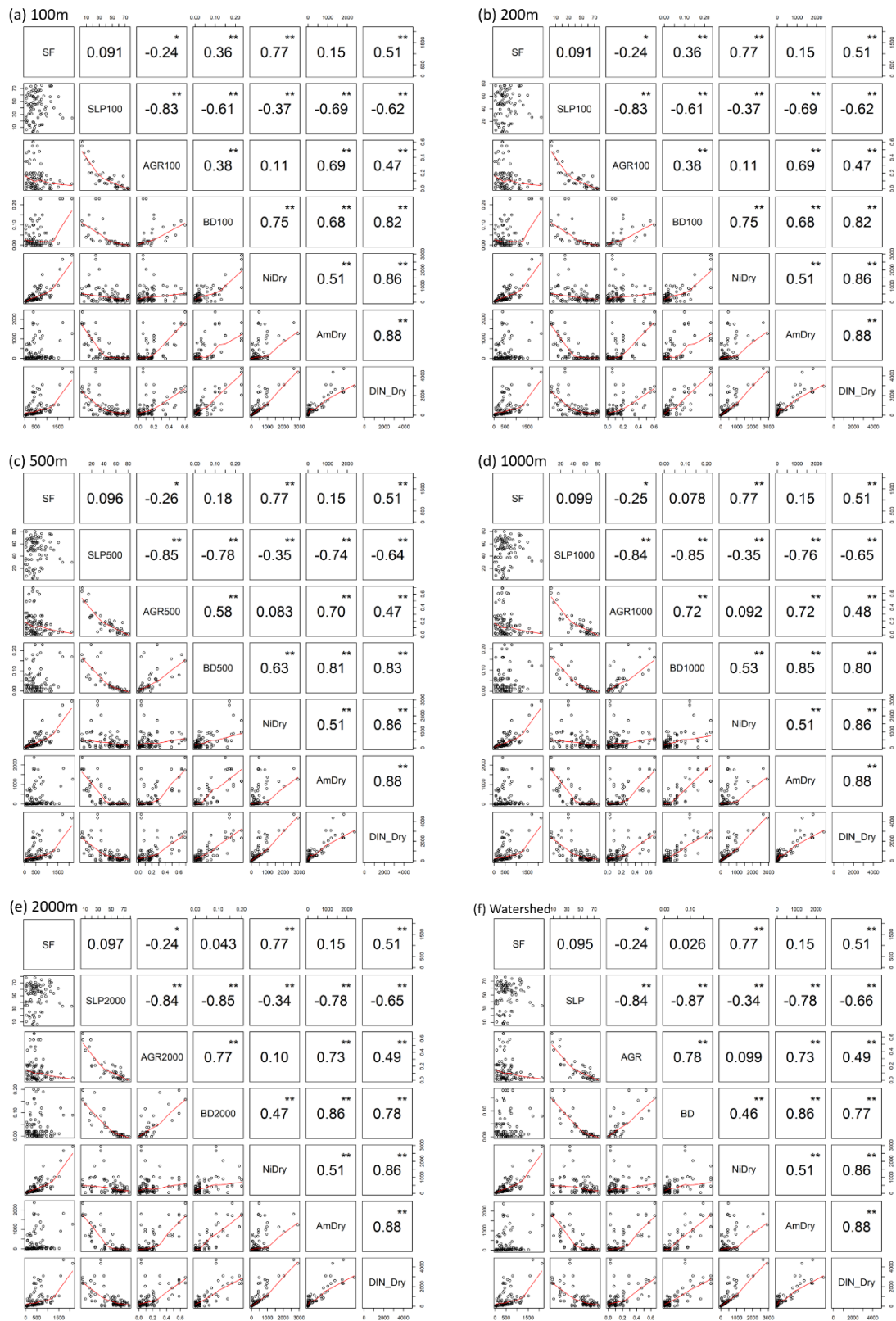
2016 Station Name	DIN			NO <sub>3</sub> <sup>-</sup>			NH <sub>4</sub> <sup>+</sup>		
	Annual	Dry	Wet	Annual	Dry	Wet	Annual	Dry	Wet
1. Wu-Tu	8969.66	4368.11	4601.55	5588.05	2917.20	2670.85	3057.74	1266.15	1791.59
2. Po-Bridge	7398.15	3091.21	4306.94	5018.76	2042.00	2976.76	2064.52	910.54	1153.98
3. San-Hsia	4087.80	1134.80	2953.00	2928.48	779.03	2149.45	1008.39	320.66	687.73
4. Hsin-Pu	2788.76	1222.67	1566.09	2358.99	1034.81	1324.18	343.33	151.50	191.82
5. Nei-Wan	2188.83	656.69	1532.14	2123.12	634.50	1488.61	56.99	19.42	37.57
6. Shang-Ping	2223.44	1059.24	1164.21	2116.83	1028.12	1088.71	95.50	25.82	69.68
7. Ping-An-Bridge	2001.76	1023.84	977.92	1784.31	903.06	881.26	145.86	84.33	61.53
8. Yun-Hsin-Chou	2233.86	1032.21	1201.65	2203.41	1017.87	1185.54	21.99	10.35	11.64
9. Pei-Shih Bridge	1839.54	983.85	855.69	1495.45	827.15	668.30	240.86	104.50	136.35
10. I-Li	1253.49	666.02	587.47	1211.64	645.61	566.03	31.00	15.28	15.71
11. Lung-An Bridge	1672.74	207.19	1465.55	1471.95	194.12	1277.83	189.57	11.96	177.61
12. Chi-Nan Bridge	6602.35	3093.40	3508.95	3997.99	1714.69	2283.29	2138.87	1164.33	974.54
13. Yu-Feng Bridge	1925.92	637.74	1288.18	1551.78	503.19	1048.59	333.45	118.68	214.77
14. Chi-Chou Bridge	2135.77	410.36	1725.42	1824.86	313.57	1511.29	263.57	85.13	178.44
15. Pei-Kang-2	8689.27	2724.01	5965.27	3381.86	841.47	2540.39	4824.23	1752.17	3072.06
16. Tun-Kun Bridge	8753.00	2383.04	6369.96	2744.42	560.30	2184.13	3432.72	1738.66	1694.06
17. Chun-Huei Bridge	3775.87	634.74	3141.13	2990.73	405.71	2585.01	727.57	209.75	517.82
18. Chu-Kuo	5845.26	558.26	5287.00	5207.82	299.54	4908.28	627.92	257.03	370.90
19. Ho-Sung Bridge	9923.87	2617.95	7305.92	5801.49	1005.11	4796.38	3290.64	1380.35	1910.30
20. Shin-Ying	6597.14	1869.92	4727.22	4533.52	958.08	3575.44	1646.04	793.90	852.14
21. Yu-Tien	2015.85	144.97	1870.88	1928.94	140.19	1788.75	58.14	2.42	55.71
22. Hsin-Shih	9866.62	2339.83	7526.79	3219.43	427.36	2792.07	5131.80	1789.08	3342.72
23. A-Lien-2	7407.47	1558.67	5848.80	3017.74	446.49	2571.26	3724.09	1013.29	2710.80
24. Chung-Te	7996.46	1416.81	6579.65	3708.44	433.94	3274.50	3587.16	880.45	2706.70
25. Li-Lin Bridge	1895.92	224.18	1671.74	1719.90	192.47	1527.43	128.42	22.39	106.03
26. Liu-Kwei	1265.41	329.55	935.86	1137.47	287.68	849.79	111.79	36.89	74.90
28. San-Ti-Men	3601.51	149.80	3451.70	3357.73	135.50	3222.23	229.15	12.85	216.29
31. Chih-Pen	1909.00	223.34	1685.66	1677.96	173.28	1504.68	206.32	39.45	166.87
32. Li-Chia	1912.49	169.83	1742.65	1843.54	161.85	1681.69	58.20	6.55	51.65
33. Tai-Tung Bridge	2530.44	460.47	2069.97	2091.88	399.07	1692.81	366.97	41.32	325.66
34. Yen-Ping	1217.58	203.61	1013.97	975.90	148.82	827.09	228.66	49.45	179.21
35. Hsin-Wu-Lu	1045.22	220.66	824.55	763.28	177.93	585.35	267.64	35.99	231.65
36. Yu-Li Bridge	1469.58	265.64	1203.94	1321.70	238.85	1082.85	134.25	23.06	111.19
37. Jui-Sui Bridge	1736.30	371.29	1365.01	1559.84	318.24	1241.60	124.73	33.30	91.43
38. His-Po Bridge	1440.55	540.30	900.24	1115.19	421.83	693.37	272.19	93.87	178.32
39. Ping-Lin	564.91	129.97	434.94	516.70	119.07	397.62	42.06	9.50	32.56
40. Jen-Shou Bridge	881.70	349.09	532.61	835.16	330.56	504.61	37.81	15.08	22.73
41. Hua-Lien Bridge	2863.30	867.02	1996.28	2577.31	789.22	1788.08	195.40	47.53	147.87
42. Lu-Shui	1655.20	426.72	1228.48	1565.33	403.51	1161.83	78.65	19.78	58.87
43. Chi-Neng-Pu	1384.30	214.63	1169.67	819.23	143.39	675.84	541.99	67.54	474.45
44. Jhong-Yue	1086.77	140.09	946.68	1036.32	133.22	903.10	43.28	5.44	37.84
45. Niu-Tou	1224.92	463.01	761.91	1186.15	447.28	738.86	29.25	12.22	17.04
46. Lan-Yang Bridge	1641.88	647.50	994.37	1381.13	547.98	833.15	216.21	79.70	136.51



**Figure S1.** Scatterplot matrix among streamflow [SF; mm], slope [SLP; %], the proportion of agriculture [AGR; %], the proportion of buildup [BD; %] of various scales and annual  $\text{NO}_3^-$ , and  $\text{NH}_4^+$ , and DIN exports at (a) 100 m, (b) 200 m, (c) 500 m, (d) 1000 m, (e) 2000 m, and (f) entire watershed scales. The asterisk indicates that the correlation is statistic significant ( $p$ -value: \*\*  $< 0.01 < * < 0.05$ ), and the red lines indicate smooth transition regressions.

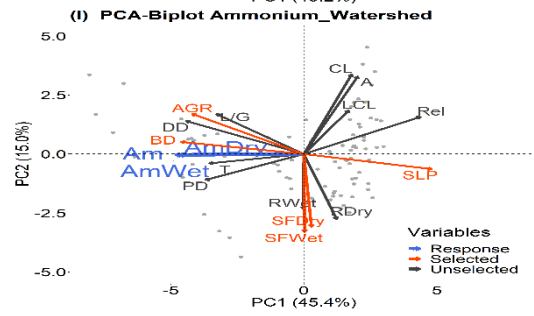
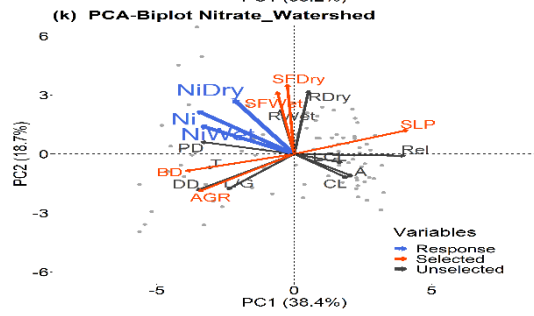
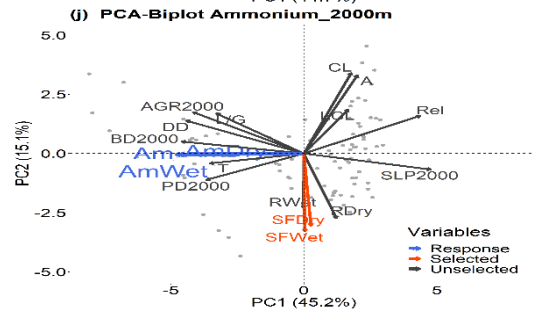
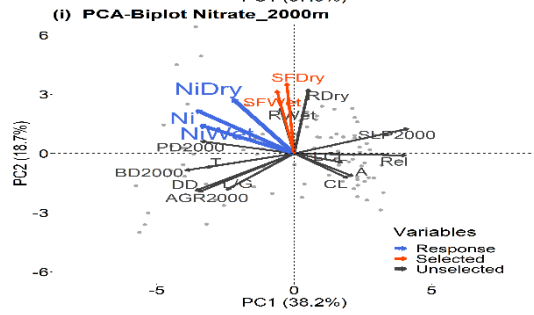
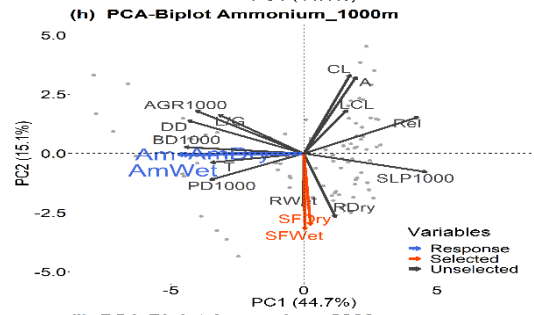
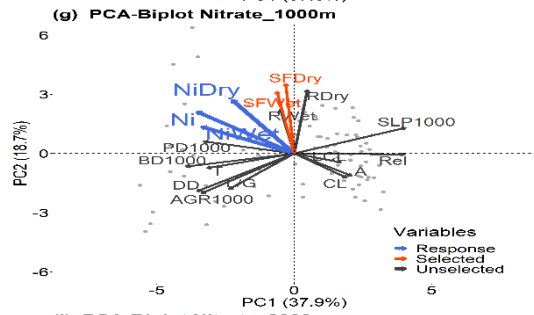
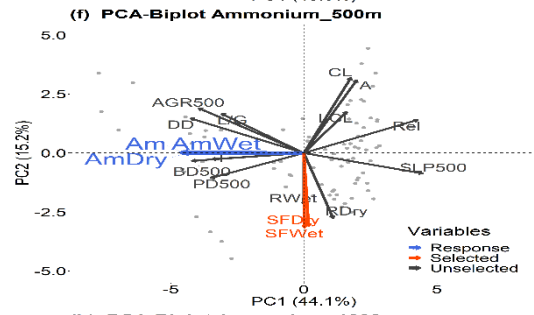
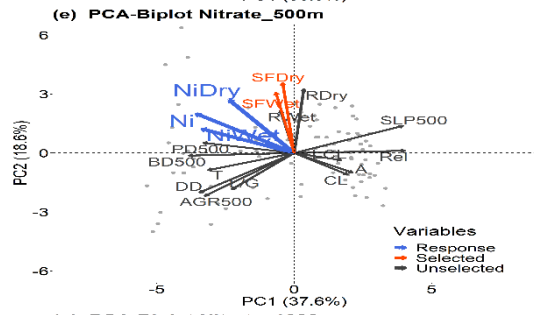
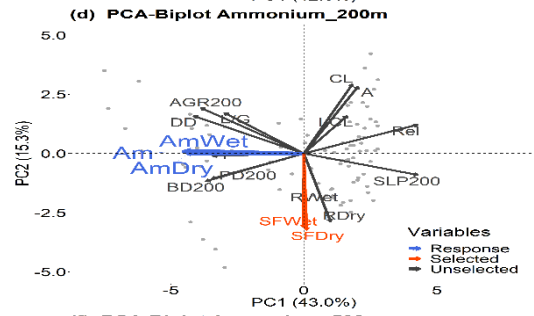
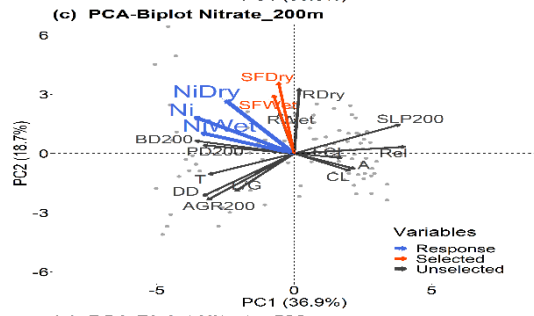
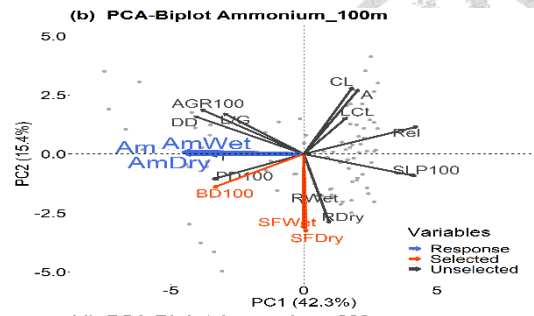
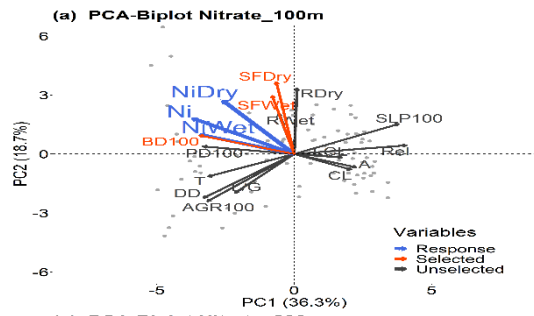


**Figure S2.** Scatterplot matrix among streamflow [SF; mm], slope [SLP; %], the proportion of agriculture [AGR; %], the proportion of buildup [BD; %] of various scales and NO<sub>3</sub><sup>-</sup> (Ni), and NH<sub>4</sub><sup>+</sup> (Am), and DIN exports during wet season at (a) 100 m, (b) 200 m, (c) 500 m, (d) 1000 m, (e) 2000 m, and (f) entire watershed scales. The asterisk indicates that the correlation is statistic significant (p-value: \*\* < 0.01 < \* < 0.05), and the red lines indicate smooth transition regressions.

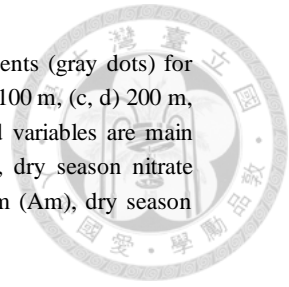


**Figure S3.** Scatterplot matrix among streamflow [SF; mm], slope [SLP; %], the proportion of agriculture [AGR; %], the proportion of buildup [BD; %] of various scales and  $\text{NO}_3^-$  (Ni), and  $\text{NH}_4^+$  (Am), and DIN exports during dry season at ((a) 100 m, (b) 200 m, (c) 500 m, (d) 1000 m, (e) 2000 m, and (f) entire watershed scales. The asterisk indicates that the correlation is statistic significant ( $p$ -value:  $** < 0.01 < * < 0.05$ ), and the red lines indicate smooth transition regressions.





**Figure S4.** Principal components analysis of environmental variables for 43 catchments (gray dots) for  $\text{NO}_3^-$  export (left panel) and  $\text{NH}_4^+$  export (right panel) at different buffer zones: (a, b) 100 m, (c, d) 200 m, (e, f) 500 m, (g, h) 1000 m, (i, j) 2000 m and (k, l) entire watershed. Red-labeled variables are main components for PC1 and PC2. Blue-labeled variables indicate annual nitrate (Ni), dry season nitrate (NiDry), and wet season nitrate export (NiWet) in (left panel) and annual ammonium (Am), dry season ammonium (AmDry) and wet season ammonium export (AmWet) in (right panel).



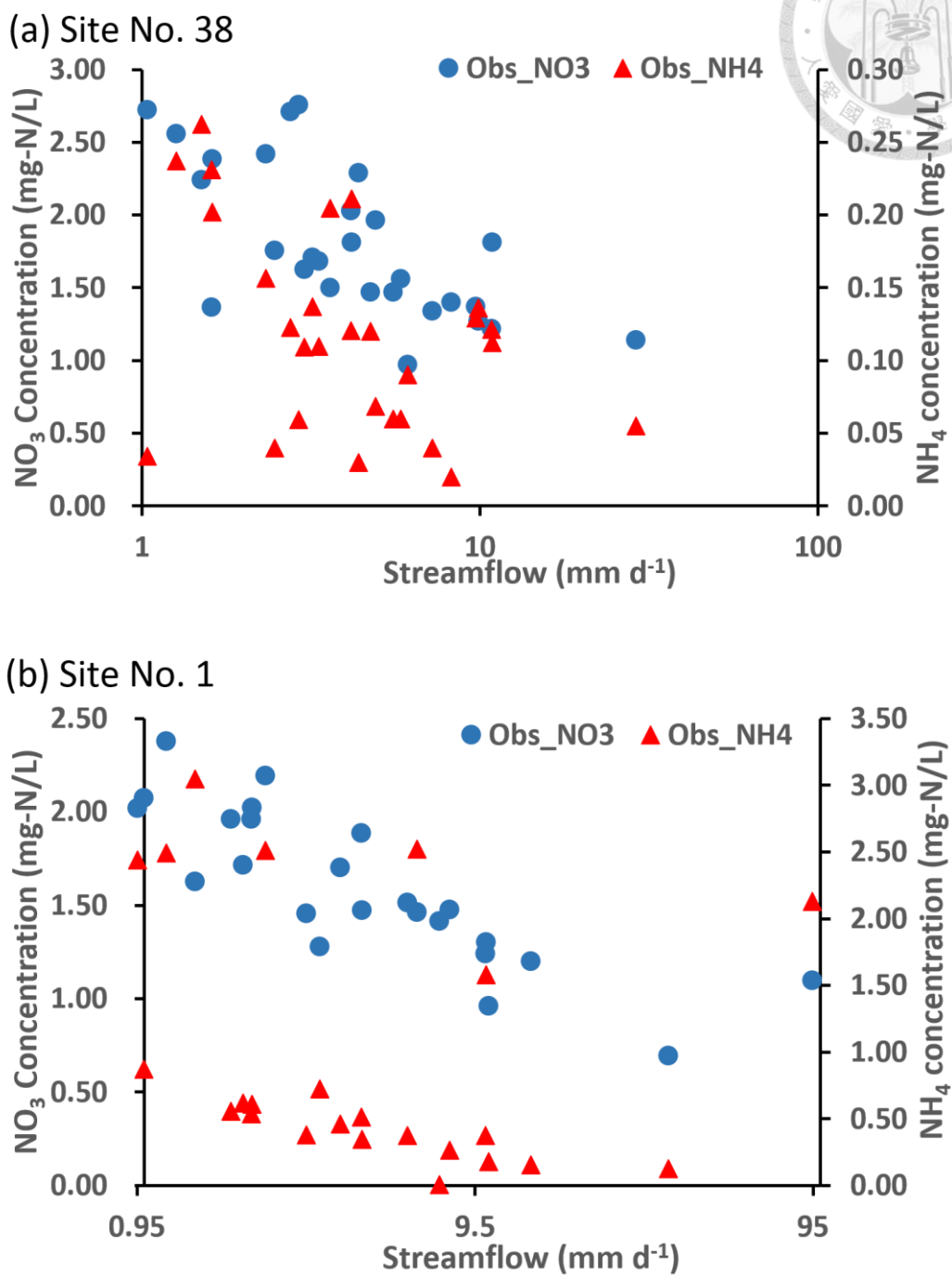
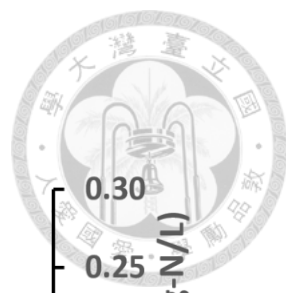


**Figure S5.** The relationship between the observed concentration (y-axis) and the simulated discharge (x-axis) in site no.38 (a) and no.1 (b) during the study period. Obs\_NO3 is the observed  $\text{NO}_3^-$  concentration; Obs\_NH4 is the observed  $\text{NH}_4^+$  concentration.